Journal of *Marine Science and Engineering*

MDPI

Article

The Optimization of a Subsea Pipeline Installation Configuration Using a Genetic Algorithm

Damir Karabaić [1,*], Marko Kršulja [1], Sven Maričić [1] and Lovro Liverić [2]

[1] Faculty of Engineering, Juraj Dobrila University of Pula, 52100 Pula, Croatia
[2] Faculty of Engineering, University of Rijeka, 51000 Rijeka, Croatia
* Correspondence: damir.karabaic@unipu.hr

Abstract: The most commonly used subsea pipeline installation method is the S-Lay method. A very important and complex task in an S-Lay installation engineering analysis is to find the optimal pipelay vessel installation configuration for every distinctive pipeline route section. Installation loads in the pipeline are very sensitive to small changes in the configuration of the pipeline supports during laying and other influential parameters, such as the tensioner force, stinger angle, trim and draft of the pipelay vessel. Therefore, the process of an engineering installation analysis is very demanding, and there is a need for an automated optimization process. For that purpose, installation engineering methodology criteria and requirements are formalized into a nonlinear optimization problem with mixed continuous and discrete variables. A special tailored multi-objective genetic algorithm is developed that can be adjusted to any desired combination of criteria and offshore standards' requirements. The optimization algorithm is applied to the representative test cases. The optimization procedure efficiency and quality of the achieved solution prove that the developed genetic algorithm operators and the whole optimization approach are adequate for the presented application.

Keywords: subsea pipeline; pipelaying vessel; pipelay analysis; optimization; genetic algorithm

check for updates

Citation: Karabaić, D.; Kršulja, M.; Maričić, S.; Liverić, L. The Optimization of a Subsea Pipeline Installation Configuration Using a Genetic Algorithm. *J. Mar. Sci. Eng.* **2024**, *12*, 156. https://doi.org/10.3390/jmse12010156

Academic Editors: Dong-Sheng Jeng and José António Correia

Received: 19 November 2023
Revised: 16 December 2023
Accepted: 8 January 2024
Published: 12 January 2024

Copyright: © 2024 by the authors. Licensee MDPI, Basel, Switzerland. This article is an open access article distributed under the terms and conditions of the Creative Commons Attribution (CC BY) license (https://creativecommons.org/licenses/by/4.0/).

1. Introduction

Subsea pipelines are an important means of continuous oil and gas transport over long distances, with great economic and geopolitical significance. The safety of the hydrocarbon supply has paramount importance nowadays. Consequently, the vulnerability and resilience of subsea pipelines to the various factors affecting their integrity and operability are receiving increased attention and attracting significant research focus [1,2]. Subsea pipeline resilience can be defined as the pipeline's capacity to withstand manmade and natural hazards, and this resilience plays a significant role in the design process [3]. These hazards could include accidental pulling with fishing gear, damages caused by terrorist activity, earthquakes, extreme climate and environmental conditions and unforeseen installation or operational loads [4–6]. The increasing demand and growth of energy consumption affect the design and installation of ever-longer subsea pipelines at increasing depths. In such conditions, the requirements of the safety, reliability and integrity of subsea pipelines become more complex.

Subsea pipeline installation is a rather complex, demanding and expensive offshore operation. Related engineering projects are driven by contradictory requirements whose optimal combination should be found. The most important are the minimization of pipeline installation loads and fatigue; minimization of residual loads in the installed pipeline; and demand for as-low-as-possible installation operation costs. Residual tension in the installed subsea pipeline is directly proportional to the applied tensioner force during installation. Minimization of residual tension is an important factor from the standpoint of increasing pipeline resilience to hazards like accidental pulling with fishing gear or the operational

hazard of damage due to vortex-induced vibrations (VIVs) in the free-span areas. That demand is, at the same time, in contradiction with the aim of minimizing installation loads, because a higher applied tensioner force decreases installation loads and vice versa. These complex requirements raise a need for an efficient optimization method of finding subsea pipeline installation configuration parameters.

A pipelay installation engineering analysis plays a pivotal role during installation project preparation. The process of laying subsea pipelines on the seabed is a very demanding operation dependent on environmental conditions. It involves careful planning and a detailed analysis in the design phase. The most commonly used subsea pipeline installation method is the S-Lay method. It is performed with S-Lay pipelay vessels; during the procedure, the pipe is controlled to bend on the seabed in the shape of the letter S (Figure 1). During the S-Lay installation, the pipeline is connected by welding on the deck of the laying ship (tubular) and is continuously lowered from the deck all the way to the seabed. The pipeline consists of a series of individual pipe elements (pipe joints) with a standard length of 12.2 m or 24.4 m, the ends of which are connected on the production line. The pipeline production line (firing line) usually contains a pipe beveling station, a pipe centering station, a few welding stations, a nondestructive testing station and at minimum one tensioning device (tensioner). The average pipeline laying capacity for most pipelay vessels is 4.5 km/day, although some vessels can set up to 7 km/day.

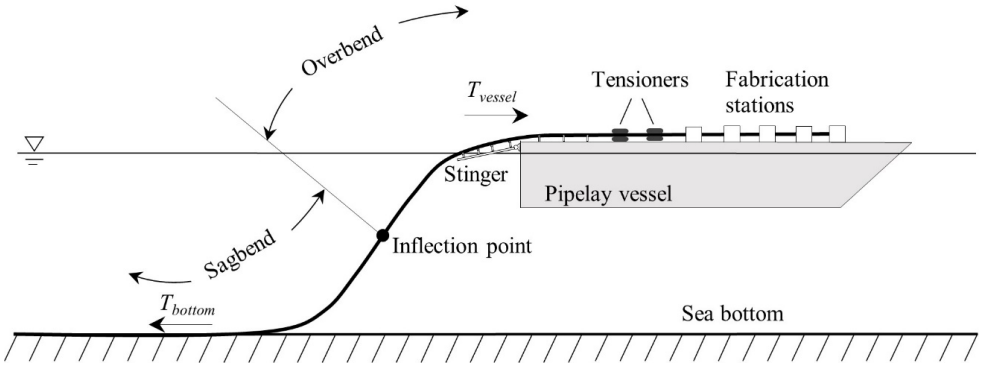


Figure 1. Subsea pipeline installation with S-lay method.

On the pipelay vessel's deck, the pipeline rests on a series of discontinuous supports, which can be rollers or track guides. Except in extremely shallow waters, as a rule, a long fixed ramp or an immersed floating strut is used (stinger), which serves to support the pipeline behind the stern of the ship as it descends into the water. A stinger is a lattice structure mounted on the ship's stern that can be attached to the vessel via a fixed or articulated link. The floating stinger is connected by a hinge and can freely float in the water. In floating freely, the stinger supports the pipe with its buoyancy force and opposes its weight. The stinger's buoyancy force, and hence its angle, can be controlled by regulating the amount of water in the stinger ballast tanks. Similar to the deck, cylindrical supports on the stinger provide a platform for the pipeline to rest upon.

After the point of separation from the stinger, the pipe extends in a long free span all the way to the point of contact with the seabed, called the touch-down point (TDP). The free span length in the S-Lay procedure typically ranges between two and three times the water depth.

To reduce stresses in the pipeline to acceptable levels, one or more tensioners are employed, transmitting a substantial tensile force to the pipeline during assembly. This tensioning action straightens the pipeline, reducing its curvature and extending the free span length. When laying in deep waters, tensile force is crucial to minimize the angle at which the pipe detaches from the stinger (Figure 1) and ensure the pipe's separation from the end of the stinger, i.e., the last support. The maximum capacity of the tensioners ranges from 50 to 750 ton-force (tf).

During pipeline installation, pipelay vessels maintain their position using a radial anchor system, typically comprising four to twelve anchor lines with winches and anchors arranged radially around the vessel. As new pipe segments are added to the assembly line, the ship advances forward by the length of the added segment. The forward movement is achieved by shortening (hauling in) anchor lines on the bow and releasing (paying out) anchor lines at the stern of the vessel. After advancing several hundred meters, it becomes necessary to reposition the anchors, which is accomplished by specially equipped boats known as anchor tugs. The anchor lines counteract the tensile force in the pipeline, keeping the ship in the desired position and mitigating environmental forces such as waves, currents and wind. Fourth-generation pipeline ships employ dynamic propulsors and a dynamic positioning system, which effectively replaces the role of anchor lines. Dynamic positioning enables pipeline installation at deeper depths where traditional anchor lines cannot be used.

Pipeline loads are highly sensitive to minor alterations in the configuration of the pipeline supports during installation. Based on the analysis results, the engineer often needs to position more than ten supports. Additionally, other critical parameters such as tensioner force, the angles of one or more stingers, pipelay vessel trim and draft must be varied. Consequently, the process of an engineering installation analysis is quite demanding, necessitating the development of an automated optimization process.

The optimization of subsea pipeline installation analysis parameters has been addressed in a limited number of research papers. The first work on this topic was Daley's paper [7], describing the graphical method for determining the optimal tensioner force based on the requirement of minimizing stinger length or on the requirement to achieve the maximum radius of curvature of the stinger supports. Maier et al. [8] optimized the articulated stinger geometry (a stinger composed of multiple floating parts jointly connected to each other) using the nonlinear programming method. Bhavikatti et al. [9] developed a method for optimizing tensioner force and free span length with the goal of minimizing the maximum bending moment in the pipeline's "S" curve. An enhanced sequential linear programming moving boundary method was utilized for optimization. Zhu and Cheung [10] presented an analytical method for analyzing a simplified S-Lay installation model with an articulated stinger, employing a singular perturbation technique. The derived analytical solution was employed to determine the optimal buoyancy combination for articulated stinger elements, albeit using an unspecified nonlinear programming deterministic method. More recent work by Ivić et al. [11] applied particle swarm multi-objective optimization to the S-Lay method installation configuration, including buoyancy tank distribution, for the installation of heavier pipelines.

In the context of applying genetic algorithms (GAs) to structural optimization problems of a similar nature, Wang and Chen [12] employed GAs to identify optimal locations for elastic vibrating rod supports, aiming to minimize vibration. Chiba et al. [13] optimized the arrangement of supports for a pipe system subjected to dynamic loads. Tabakov in [14] presents an overview of multi-criteria optimization of layered structures using GA. Vieira et al. [15] applied GA to optimize the configuration of vertical submarine pipes (risers) and in [16] they compared this application of GA to other optimization algorithms inspired by biological processes. Gantovnik [17] provides an overview of GAs adapted for the optimization of composite structures.

A significant number of studies have explored the application of GA optimization in offshore engineering. Shafieefar and Rezvani [18] demonstrate the optimization of anchor lines for floating oil platforms utilizing GA, while Boulougouris and Papanikolaou [19] apply GA to multi-criteria optimization of floating LNG terminals. Clauss and Birk investigated the optimization of the hydrodynamic form of general large marine structures using the tangent search method in [20,21], and then compared the efficiency of optimization with the sequential quadratic programming deterministic method on a similar problem. In [22], Lee and Clauss present a method of automated design of the shape of a floating

marine structure with the objective of minimizing motion induced by sea waves. They performed shape optimization using the adaptive simulated annealing method.

Subsea pipeline design is inextricably linked to and dependent upon subsea pipeline installation engineering. A series of studies have been conducted on the topic of subsea pipeline route optimization utilizing GA and the development of associated software tools—de Lima Jr. et al. [23], Baioco et al. [24], de Lucena et al. [25] and Baioco et al. [26].

Among recent studies addressing offshore engineering problem optimization with GA are Kim et al. [27], who explored the design of an underwater chain trencher based on GA optimization. Liu et al. [28] employed hybrid algorithms to optimize the offshore wind turbine jacket substructure. Ghigo et al. [29] conducted platform optimization and a cost analysis in a floating offshore wind farm. Yin et al. [30] optimized static and discrete berth allocation for large-scale marine-loading problems using an iterative variable grouping GA. Zhang et al. [31] employed GA optimization to optimize configuration parameters of a new energy hybrid system. Sun Q. et al. [32] performed optimization of the anchor chain design of a catenary anchor leg mooring system. Sun H. et al. [33] optimized the number, hub height and layout of offshore wind turbines using GA.

The first research objective of this study was to systematically analyze and standardize the process of a subsea pipeline installation analysis. To achieve this goal, installation engineering methodology criteria and requirements were formalized into a nonlinear optimization problem involving both continuous and discrete variables.

The second research objective was to develop a complete optimization procedure based on a genetic algorithm (GA) that would enable the automated discovery of the optimal combination of all crucial parameters of subsea pipeline installation configuration, characteristic for the S-Lay method. Optimization using a genetic algorithm specifically designed for this problem should meet all the requirements that are set when analyzing and determining the configuration of the pipelaying procedure in practical project implementation.

A specifically designed multi-objective genetic algorithm is created that can be customized to suit any prescribed combination of criteria and offshore standards' requirements for subsea pipeline installation with the S-Lay method. The optimization algorithm is applied to the representative test cases. The effectiveness of the optimization procedure and quality of the obtained solution demonstrate that the developed genetic algorithm operators and whole optimization approach are suitable for the given optimization problem and application.

2. Materials and Methods

The development of multi-objective GA for S-Lay installation configuration optimization (Section 3) was founded on the following four methodological components, which are detailed in this section:

- An S-lay installation method analysis;
- Subsea pipeline installation analysis methodology;
- Optimization problem formulation;
- Genetic algorithm optimization.

2.1. S-Lay Installation Method Analysis

On the production line, where pipeline segments are connected, the pipeline layout can be considered nearly horizontal and parallel to the water surface (Figure 1). At the stern, where the pipe transitions into the water, the deck and pipe supports descend at a slope to ensure that the pipe enters the water at a defined angle. Pipe supports are typically configured to allow the pipe to bend downwards with a specific curvature radius. This applies to supports on both floating stinger and fixed ramps. Due to this curvature, the pipe adopts a specific separation angle from the stinger. Consequently, the stinger angle should be at least equal to the separation angle to prevent excessive pipe bending over the last support on the stinger, leading to excessive stresses at that point.

The "S" curve features an inflection point dividing it into two curvature regions:

- Overbend—the initial section of the "S" curve, spanning the supports on board and the stinger. The pipeline curve $y = f(x)$ is concave ($y'' < 0$);
- Sagbend—the terminal section of the "S" curve extending to the seabed. The pipeline curve is convex ($y'' > 0$).

The inflection point is usually found immediately after the stinger's end, specifically after the last stinger support. At this point, the bending moment is zero and undergoes a sign change, as does the curvature, which, according to the Euler–Bernoulli beam theory, is linearly proportional to the bending moment.

In relatively shallower water depths and with larger-diameter pipes, the shape of the "S" curve of the pipeline is relatively gentle and is principally determined by the pipe's bending stiffness. The behavior of the pipe in the free span, that is, in the sagbend, resembles that of an elastically supported linear rod. Conversely, in deeper water depths and with smaller-diameter pipes that exhibit relatively low bending stiffness, the pipeline's behavior approximates that of a catenary model. The pipe's curvature is more pronounced and is predominantly determined by the tensioner's force.

Upon reaching the end of the sagbend region, the pipe comes into contact with the seabed at the TDP. If the seabed is relatively flat, the pipe can be regarded as lying on the seabed in an undeformed state, provided that residual tensile stress caused by the tensioner's force and bending near the contact point is disregarded. At a specific distance of approximately 100 m from the TDP, there is a point of apparent fixation of the pipeline, beyond which the pipeline's condition can be considered to be consistent and unaffected by the installation process.

Static stresses in the pipe within the overbend region are primarily influenced by four key parameters:

- Common radius of curvature corresponding to the supports' configuration;
- Pipe free span weight between the supports;
- Bending torque local increase over supports;
- Axial pipe tensile force generated by the tensioner force.

These stresses are highly sensitive to changes in the height of the roller supports. The relatively short distance between the supports amplifies the impact of even small changes in support height.

The primary factors affecting static stresses in the pipe in the sagbend region are

- Tensioner force;
- Pipe weight in the free span;
- Free span length.

Since the primary influencing factors that determine static stresses in the pipeline's overbend and sagbend regions operate in the vertical plane, the static analysis of laying pipelines can be simplified to a two-dimensional (2D) problem. A three-dimensional (3D) analysis is typically required only when laying pipelines along a winding route, where a detailed analysis of the ship's curved laying path is necessary. In practice, the pipe bends more significantly over the supports than between them, leading to a typical increase in strain over the supports and decreases in strain between them.

Research and development of mathematical models and corresponding solutions for subsea pipelines' S-Lay installation method began with the rise of the subsea pipeline construction industry in the 1960s. First, published models were limited to simulating pipe stresses in the unsupported sagbend area [34–38]. Subsequent advancements led to the development of more sophisticated models that incorporated geometric and material non-linearities, fully modelled the overbend region with supports and accounted for dynamic environmental loads [39–51].

The most suitable model for analyzing static pipe stresses during S-Lay pipelay operation is a simplified one-dimensional homogeneous tensed rod subjected to its own weight

and large deflections (geometrical nonlinearity), described using Euler–Bernoulli beam Equation (1) [52–57]:

$$T(s)\frac{d\theta}{ds} - EI\frac{d^3\theta}{ds^3} - w(s)cos(\theta) = 0, \quad (1)$$

where

$T(s)$—Tensile (axial) force component in an arbitrary pipe section;
s—Curvilinear coordinate;
θ—Slope of the pipe curve;
E—Young modulus of elasticity;
I—Moment of inertia of the pipe cross section;
$W(s)$—weight of the pipe in an arbitrary pipe section.

Upon introducing Equation (2) for the horizontal force component $H(s)$ in an arbitrary pipe section,

$$H(s) = T(s)cos(\theta) + F(s)\,sin(\theta), \quad (2)$$

where

$F(s)$—Shear force in an arbitrary pipe section.

Nonlinear beam bending Equation (3) can be derived in a form commonly found in relevant literature [49,51,52]:

$$EI\frac{d}{ds}\left[sec(\theta)\frac{d^2\theta}{ds^2}\right] - H(s)sec^2(\theta)\frac{d\theta}{ds} + w(s) = 0. \quad (3)$$

Equation (3) is applicable to both shallow and deep waters and for small and large displacements. It is a third-order nonlinear differential equation with an unknown pipe length in the free span and an unknown sea bottom reaction force at the free end. This distinctive characteristic makes pipelaying problems more challenging to solve than classical nonlinear beam models and allows the formulation of the problem as either an initial value problem (IVP) or a boundary value problem (BVP). Equation (3) can also be expressed in terms of the function $y(s)$ instead of $\theta(s)$.

Some earlier research works introduced the solution of Model (3) as an IVP [34,36], where initial values of $\theta(s)$ or $y(s)$ and their derivatives are specified at one fixed pipe end, typically the tensioner end or TDP. An advantage of the IVP approach is that it eliminates the need for an additional boundary equation to determine the unknown pipe span length. However, a major drawback of the IVP approach is its inability to converge for nonlinear problems in general. This has led to the adoption of the more robust BVP approach in recent models. The BVP solution necessitates three boundary conditions (BCs) to be defined. Assuming a fixed pipelay vessel, typically at the tensioner end ($s = 0$), two BCs are established, zero rotation $\theta(0) = 0$ or vertical displacement $y(0) = 0$, along with tensioner force $T(0) = T_0$. The third BC is specified at the free pipe end, where a vertical displacement of $y(L) = -D$ is defined, corresponding to the depth of the seabed D. In addition to the three BC, an additional boundary equation is required to determine the unknown elastic line free span length L. Furthermore, the arbitrarily supported pipe in the overbend and at the TDP end can be generally described using a supporting vertical displacement constraint function, $y_{svdc}(s)$. The specific form of this function depends on the model, vessel and stinger geometry. The conventional approach is to assume perpendicular contact reactions between the pipe and the supports. Various combinations of BCs can be employed to close the BVP.

Nonlinear beam bending Equation (3) can only be solved analytically with certain simplifying assumptions [42,47]. Numerical methods are necessary to solve the full Equation (3) in conjunction with the general supporting vertical displacement constraint function $y_{svdc}(s)$. The most accurate results are obtained using the finite element method (FEM) with beam elements specifically designed to handle large displacements (geometrical nonlinearity) [36].

Dedicated finite element software packages are employed for a subsea pipeline installation engineering analysis in the offshore construction industry. These packages can effectively model and analyze problems involving various components, including rigid, slender and flexible elements such as pipes, tubular members, flexible risers and cables, under static and dynamic loads. Offpipe software [58] stands as a prominent industry standard for static and dynamic pipelay analyses, having been extensively used in numerous worldwide projects over the years. It is based on the finite element method described in [40]. Offpipe employs specialized finite element models of the entire pipeline system, encompassing the pipelay vessel, pipe supports, stinger and seabed. The software can handle both 2D and 3D analyses and perform a dynamic analysis for single or multiple simultaneous sea states, including regular and random waves. Other widely used general offshore construction analysis software packages for a pipelay installation analysis include Orcaflex by Orcina Ltd. [59] and Flexcom by Wood Group Kenny [60].

The same model can be analyzed and solved using general-purpose nonlinear finite element analysis (FEA) computer-aided design (CAD) software packages such as SIMULIA Abaqus by Dassault Systèmes [61], Ansys Mechanical by Ansys Inc. [62] and Autodesk Inventor Nastran [63]. However, specialized software solutions specifically designed for a pipeline installation analysis are more efficient in handling the large number of parameters involved in a pipelay installation analysis and provide faster solver speeds due to their reduced model complexity. Ivić et al. [64] implemented and solved an S-Lay pipelaying model using SIMULIA Abaqus 6.11 [61] and validated the results with standard pipelay analysis software Offpipe v2.05. The static subsea pipeline installation methodology and optimization method described in the following sections are independent of the specific pipelay installation analysis software used. In this research, Offpipe software v2.07 [58] was employed as the S-Lay method static analysis solver for the implemented genetic algorithm optimization method.

2.2. Subsea Pipeline Installation Analysis Methodology

During the static installation analysis of the S-Lay pipelay method, a large number of parameters need to be optimized to determine their optimal combination that enables safe laying operation with minimal execution time, ultimately minimizing the entire operation costs. The engineering analysis of S-Lay pipeline installation typically involves evaluating static pipeline loads along the "S" curve, including tensile force, bending, pressure, contact forces on supports and contact forces on the seabed. This analysis aims to determine the optimal S-Lay static laying configuration.

The overbend curvature of the "S" curve is influenced by the stinger angle and the configuration (heights) of the supports on the pipelay vessel and stinger. The tensioner force affects the sagbend curvature of the "S" curve and the bending moment at the stinger tip. The required tensioner force is dependent on the water depth, immersed pipe weight, permissible overbend radius of curvature, pipe–stinger separation angle and permissible sagbend radius of curvature.

Key parameters of the S-lay pipelay method configuration that are adjusted during an installation analysis are depicted in Figure 2. Detailed parameter descriptions are provided in Section 2.3. The water depth and pipe weight are determined by pipeline design and therefore are not considered as optimizable parameters during an installation analysis.

A primary objective of pipelay configuration parameter optimization is to fulfill the project criteria. These criteria are established to safeguard the pipeline's integrity during the laying process and ensure that the installation equipment adheres to its operational limitations as defined for the specific project.

Design criteria for ensuring pipeline integrity are established by industry regulations. The DNV-ST-F101 standard "Submarine pipeline systems" [65] is the most widely used and relevant design criterion for pipeline installation projects, making it the basis for defining, testing and calibrating the genetic algorithm optimization. Other criteria essentially involve similar combinations of the permissible bending moment or equivalent strain and

permissible deformation in the overbend and sagbend. Therefore, the flexible ability to define the project criteria enables optimization based on any of these criteria as described in the following sections. To accommodate the variations in overbend and sagbend criteria, a flexible approach has been adopted that allows setting both the permissible static bending moment and the permissible deformation in both the overbend and sagbend.

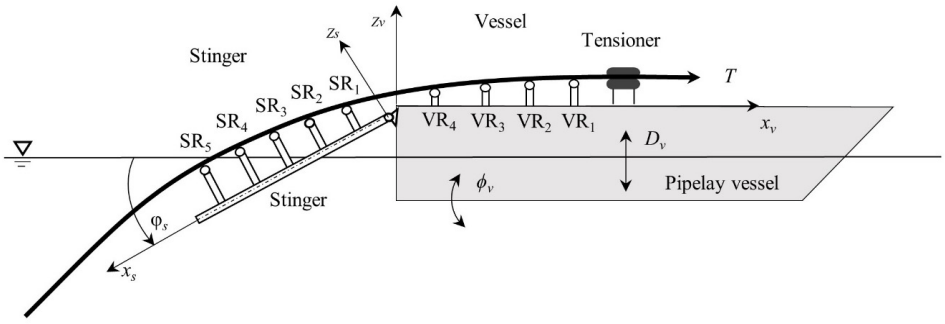


Figure 2. Subsea pipeline S-Lay installation method configuration parameters.

Operational limitations of installation equipment include permissible loads (reactions) on pipe supports (vessel and stinger), maximum applicable tensioner force and stinger ramp angle restrictions.

The DNV-ST-F101 standard [65] design criterion establishes distinct criteria for permissible combined loads based on the division into two regions:

1. Displacement controlled condition (DCC) region—pipeline deformation and the position of the "S" curve are primarily determined by the placement of supports and stingers, making them geometrically conditioned. The criterion prescribes a maximum allowable total strain, $\varepsilon \leq \varepsilon_{allow}$, at all evaluated points (nodes) within the overbend. This calculated allowable installation strain represents unique input data for each pipeline section. The standard value is ε_{allow} = 0.002 (0.2%). While this region is often incorrectly referred to as the overbend in engineering practice, this terminology will be retained for consistency. However, the boundary between the overbend and sagbend is defined by the inflection point of the "S" curve (see Figure 1);
2. Load controlled condition (LCC) region—pipeline deformation and position of the "S" curve are primarily determined by the tensioner force; therefore, they are conditioned by the loads on the pipeline. The criterion prescribes a maximum allowable bending moment, $M_b \leq M_{allow}$, at all evaluated points (nodes). This region is also often imprecisely labeled as the sagbend, although it encompasses the area above the inflection point. Therefore, this work will further distinguish between the sagbend(+) region above the inflection point of the "S" curve with a positive bending moment and the sagbend(−) area below the inflection point with a negative bending moment.

The boundary between the DCC and LCC regions is typically situated before the last support on the pipelay vessel or the fixed ramp preceding the articulated connection with the floating stinger. Consequently, the exact position of this boundary varies depending on the type of the stinger ramp attached, rigid or floating. For the pipelay vessel depicted in Figure 2, if the stinger is rigid, the last support within the DCC region would be SR4. In the case of a floating stinger, the last support within the DCC region would be VR3. The bending moment allowance criterion for the LCC region is generally more conservative and is sometimes applied in the sagbend region.

2.3. Optimization Problem Formulation

The objective of static laying analysis optimization is to determine the optimal combination of parameters that define the S-Lay installation method configuration, ensuring that all project criteria are satisfied. The entire configuration can be characterized by a set of invariant (fixed) parameters and a set of variable parameters.

Invariant parameters are unique to each section along the pipeline route and establish the optimization environment as a set of variable states during the laying process. This group comprises parameters that serve as input variables for static pipelay analysis software and are derived from pipeline properties along the route:

1. Water depth;
2. Outer pipeline diameter;
3. Pipe wall thickness;
4. Pipe weight in air;
5. Submerged pipe weight;
6. Pipe steel material Specified Mean Yield Stress (SMYS);
7. Pipe equivalent Young modulus of elasticity (accounting for concrete coating if applicable).

Variable parameters are those whose values need to be determined during the optimization (optimized parameters) and can be categorized as follows (Figure 2):

1. Pipelay vessel parameters:
    a. Tensioner force (T);
    b. Supports' configuration (VR1. . .VR4 supports' height arrangement);
    c. Trim (angle of inclination ϕ_v);
    d. Draft (D_v).
2. Stinger parameters:
    a. Supports' configuration (SR1. . .SR5 supports' height arrangement);
    b. Stinger angle (φ_s).

Optimization conditions are classified into two categories based on the requirement to fulfill them at the end of the optimization process: mandatory and additional optimization conditions.

Mandatory optimization conditions—compliance with these conditions is mandatory and serves as the foundation for establishing optimization constraint functions and defining the overall optimization process. These mandatory optimization conditions are derived from the previously described static laying analysis criteria:

- Meeting the pipeline integrity criteria;
- Meeting the installation equipment operational limiting criteria.

Additional optimization conditions—the optimization process should aim to fulfill these conditions to the greatest extent possible, but they are not mandatory. Most of these conditions serve as the foundation for defining an optimization goal function. When multiple goals are defined, the optimization problem becomes multi-objective and each goal (criterion) should have a corresponding goal weighting factor that reflects its relative importance compared to others. Optimization based on these conditions can be customized based on the specified weight inputs. Additional optimization conditions include

- Minimization of maximum values for defined pipeline integrity criteria, e.g., the maximum value of bending, stress or deformation moment at any finite element node within overbend or sagbend regions;
- Minimization of maximum values for defined operational limiting criteria of installation equipment, e.g., the maximum reaction force value at any support;
- Uniform distribution of support reaction forces: minimizing the deviation of supports' reaction forces from their mean value while avoiding situations where supports are not in contact with the pipe;
- Uniform distribution of load on supports—minimizing of load deviation at individual supports from their mean value;
- Minimum required tensioner force application.

The optimization of a subsea pipeline S-Lay installation configuration falls under the category of general nonlinear optimization problems (Rao [30]). This problem is characterized by a combination of continuous and discrete variables, a nonlinear objective function and nonlinear constraint functions. Both the objective function and constraint

functions are not expressible in an analytical form but rather represent the outcomes of a numerical simulation of the laying process.

The constrained nonlinear optimization problem can be formulated as follows:

Find the vectors $X^* = (x_1^*, x_2^*, \ldots, x_m^*)^T$ and $Y^* = (y_1^*, y_2^*, \ldots, y_n^*)^T$ that minimize the objective function

$$f(X^*, Y^*, P, R) = \min [f(X, Y, P, R)], \quad (4)$$

subject to the constraints

$$g_k(X^*, Y^*, P, R) \geq 0, \qquad k \in \{1, \ldots, r\}, \quad (5)$$

$$h_l(X^*, Y^*, P, R) = 0, \qquad l \in \{1, \ldots, s\}, \quad (6)$$

and the given upper and lower bounds for the optimization variables

$$(X_i)_{min} \leq X_i \leq (X_i)_{max}, \qquad i \in \{1, \ldots, m\}, \quad (7)$$

$$(Y_j)_{min} \leq Y_j \leq (Y_j)_{max}, \qquad j \in \{1, \ldots, n\}, \quad (8)$$

where

$f(X, Y, P, R)$—objective function;
$X = (x_1, x_2, \ldots, x_m)^T$, $X \in \mathbb{R}^m$—the vector of real (continuous) optimization variables;
$Y = (y_1, y_2, \ldots, y_n)^T$, $Y \in \mathbb{Z}^n$—the vector of integer (discontinuous) optimization variables;
$P = (p_1, p_2, \ldots, p_p)^T$, $P \in \mathbb{R}^p$—the vector of invariant real parameters;
$R = (r_1, r_2, \ldots, r_q)^T$, $R \in \mathbb{Z}^q$—the vector of invariant integer parameters;
$g_k(X, Y, P, R) \geq 0$—inequality constraint functions;
$h_l(X, Y, P, R) = 0$—equality constraint functions;
m—the number of real optimization variables;
n—the number of integer optimization variables;
r—the number of constraint functions in the form of inequality;
s—the number of constraint functions in the form of equality;
p—the number of invariant real parameters;
q—the number of invariant integer parameters.

Each equality constraint function can be replaced by two inequality constraint functions, thereby eliminating the need for Equations (5) and (6) and replacing them with Equation (9):

$$g_k(X^*, Y^*, P, R) \geq 0, \qquad k \in \{1, \ldots, r + 2s\}. \quad (9)$$

2.4. Genetic Algorithm Optimization

The optimization of a subsea pipeline S-Lay installation configuration falls into the category of challenging nonlinear optimization problems. The nonlinear objective function and constraint functions are derived from numerical simulation of the S-Lay installation method, making them unavailable in analytical form. Consequently, first- and second-order derivatives, which are crucial for gradient-based optimization methods, must be estimated using approximate techniques, such as the finite difference method. This necessitates at least two pipelay simulations for each partial derivative of the objective function and each optimization parameter.

Standard nonlinear programming methods (gradient and others) would be inefficient for this problem, demanding excessive computational resources and often finding local optima near the starting point. Heuristic optimization methods are better suited for such nonlinear problems, as they employ a directed random search to find the global optimum. Genetic algorithms have demonstrated efficacy in solving such problems, often identifying globally optimal solutions with high probability.

A genetic algorithm (GA) is an algorithm that utilizes a directed heuristic, stochastic search method inspired by natural evolution (refs. [66–72]). Natural evolution relies on a selection process that prioritizes the survival of the most exceptional (best) individuals

within a particular species. The operators of a genetic algorithm operate on individuals within a population over multiple generations, striving to progressively enhance their quality (fitness). Individuals that represent potential solutions are frequently compared to chromosomes and are represented using strings or binary numbers. Similarly to other heuristic methods (e.g., simulated annealing), a genetic algorithm should find a global minimum even when the objective function has multiple extremes, including local maxima and minima. A general genetic algorithm flowchart is depicted in Figure 3.

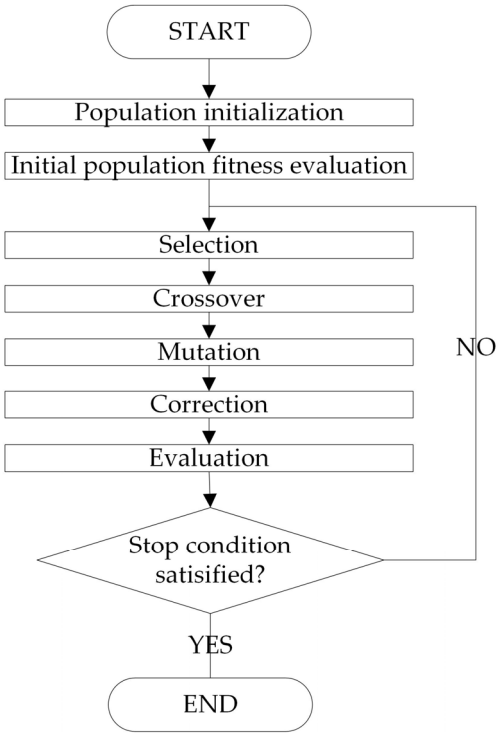


Figure 3. Genetic algorithm flowchart.

The stop condition for GA optimization can be based on the maximum number of generations, the fitness function limit, the change in the best fitness function tolerance or other criteria. The stop condition is typically defined as a combination of these criteria.

A chromosome represents an individual within a genetic algorithm, encapsulating the values of optimization variables. To simplify representation, variables are not encoded in their decimal form but rather as integer values that represent discretized real values between the minimum and maximum for a specified discretization step. An optimization variable is often referred to as a gene.

A population is a set of solutions representing the current iteration step (generation) of a genetic algorithm. Population size is a crucial parameter in GAs and its accurate determination is essential. If the population size is too small, the genetic algorithm may converge prematurely; if it is too large, the genetic algorithm unnecessarily consumes computing resources, and the time required to improve the solution may be unnecessarily prolonged. Two critical concepts emerge in the evolutionary process and genetic search: population diversity and selective pressure. Both factors are significantly influenced by population size. Population size flexibility can be relatively easily implemented within a GA.

At each successive generation, a portion of the existing population is selected to create a new generation. Individual solutions are chosen through a fitness function process, favoring those with higher fitness values. Some selection methods evaluate the quality of each solution and select the best solutions based on direct comparison. Others perform assessments on a random sample of the entire population to expedite the process.

Many selection mechanisms are stochastic and are designed to select a small percentage of inferior solutions. This practice helps maintain population diversity, preventing premature convergence toward inferior solutions. Among the most renowned selection algorithms are simple selection (roulette wheel), proportional selection and tournament selection.

The most crucial role of crossover is to combine distinct chromosomes (individuals) and transmit their genes to a new population [66]. For each new solution to be generated, a pair of (parental) solutions are chosen from a pre-selected set for reproduction. The creation of a "child" (or "offspring") employing the crossbreeding and mutation yields a novel solution that typically incorporates novel characteristics of its "parents". New parents are selected for each child and the cycle continues until a new population of appropriately sized solutions is created.

Mutation is essential because the population cannot encompass all possible genes and there must be a mechanism for introducing new genes that could potentially represent optimal solutions or serve as valuable stepping stones toward the optimum. In a genetic algorithm, mutation serves as a mechanism for maintaining population diversity.

Similar to crossover, mutations are not applied with every iteration. The probability of mutation is typically set to a low value, often below 0.05 for binary-encoded chromosomes. However, for integer coding and floating-point encoding, the mutation probability can be significantly higher, ranging up to 0.8.

3. Multi-Objective Genetic Algorithm for S-Lay Installation Configuration Optimization

A multi-objective GA is developed to achieve the goal of creating a flexible automated algorithm that adheres to the guidelines of the subsea pipeline installation analysis methodology outlined in Section 2.2.

The GA's stop condition combines two termination criteria and the algorithm terminates when either of the following criteria is met:

1. No improvement in the best individual's fitness value for a predetermined number of generations, with a specified fitness function value tolerance;
2. The maximum number of generations has been reached.

3.1. Chromosome Encoding

A chromosome represents an individual in the genetic algorithm and encapsulates the values of optimization variables. For simplicity, variables are not encoded in decimal form but are represented as integer values that discretize the real-valued range between the minimum and maximum for the specified discretization step. Optimization variables are commonly referred to as genes. The mathematical representation of the general form of the solution (chromosome) is a vector denoted by $X = (x_1, x_2, \ldots, x_m)^T$. Figure 4 depicts the chromosome encoding employed for pipelay configuration optimization, corresponding to the pipelay vessel defined for the test cases presented in Section 3.

3.2. Fitness Function

Fitness represents a relative assessment (relative to the average or best chromosome) of chromosomes. The fitness function serves as a mechanism for evaluating chromosome quality. To optimize pipeline laying, a multi-objective function is employed and constrained GA optimization is implemented using the penalty function approach [73]. Constraints are defined as permissible limits on maximum stresses in the pipeline (bending moment, relative stress or deformation) and/or permissible reaction forces on supports. The fitness function for constrained multi-objective optimization with the application of the penalty function is defined as

$$f(X) = O(X) + P(X), \tag{10}$$

where

$O(X)$—Multi-objective goal function to be minimized;

$P(X)$—Penalty function.

Parameter	Value	Chromosome
VR1	7.0	20
VR2	5.6	16
VR3	3.9	19
VR4	2.0	10
SR1	3.3	23
SR2	3.7	17
SR3	3.9	24
SR4	3.8	18
SR5	3.4	24
Tensioner force	50	7
Stinger angle	17	17
Trim	−1.1	8
Draft	9.1	31

Figure 4. Chromosome integer encoding for pipelay configuration optimization.

To streamline selection method implementation, the fitness function is transformed into an absolute fitness function that needs to be maximized:

$$F(X) = \frac{1}{f(X)}. \tag{11}$$

The nonlinear multi-objective goal function and the nonlinear penalty function are calculated based on the results of the pipeline S-Lay installation method static analysis simulation, making them unavailable in analytical form. A flowchart outlining the genetic algorithm fitness function evaluation process is presented in Figure 5.

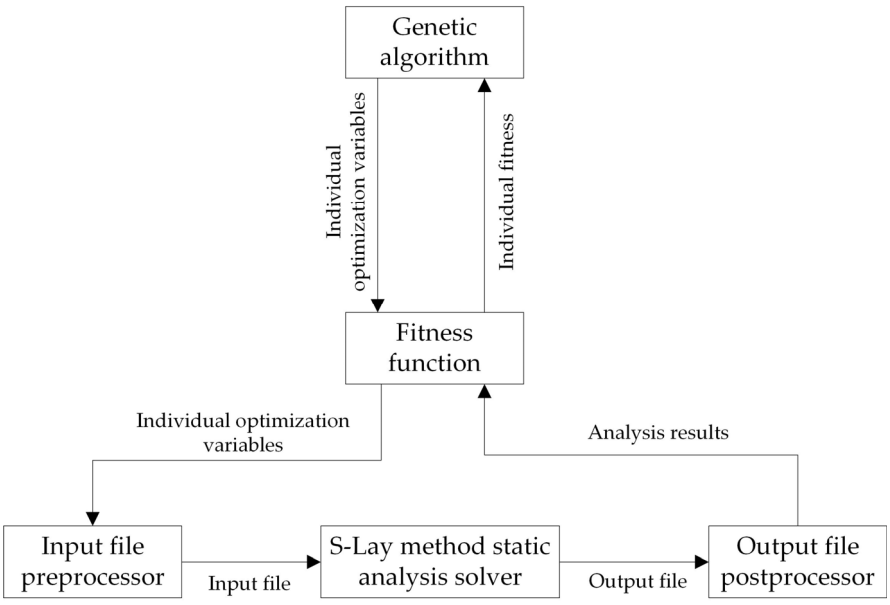


Figure 5. Genetic algorithm fitness function evaluation flowchart.

3.3. Objective Functions

Optimization objectives are related to the loading condition of the pipe (or support) and can be applied to the entire length of the pipe or specified for distinctive regions of

the pipe (overbend, sagbend). The multi-objective goal function is formulated as a sum of weighted objective functions:

$$O(X) = \sum_{i=1}^{N_O} ow_i \cdot o_i(X), \tag{12}$$

where

N_O—number of objectives;
o_i (X)—objective function;
ow_i—i-th objective function weight factor, where

$$\sum ow_i = 1, \tag{13}$$

The weighting factor approach enables flexible customization of pipelay analysis criteria tailored to specific offshore construction standards' requirements. Unnecessary criteria can be readily disabled by setting their weighting factor as equal to zero while adjusting the remaining factors to ensure compliance with Equation (13).

Pipelay analysis criteria that can be independently configured for the overbend and sagbend include

1. Allowable bending moment—M_{b_allow};
2. Allowable relative stress—equivalent stress and SMYS ratio—σ_{rel_allow};
3. Allowable deformation—ε_{allow}.

The objective function that minimizes the maximum overbend bending moment is

$$o_1(X) = \frac{M_{b_max_OV}(X)}{M_{b_allow_OV}}, \tag{14}$$

where

$M_{b_max_OV}$—maximum overbend bending moment;
$M_{b_allow_OV}$—allowable overbend bending moment.

The objective function that minimizes maximum overbend relative stress is

$$o_2(X) = \frac{\sigma_{rel_max_OV}(X)}{\sigma_{rel_allow_OV}}, \tag{15}$$

where

$\sigma_{rel_max_OV}$—maximum overbend relative stress calculated from Equation (16),

$$\sigma_{rel_max_OV}(X) = \frac{\sigma_{e_max_OV}(X)}{\sigma_0}, \tag{16}$$

$\sigma_{e_max_OV}$—maximum overbend equivalent Von Mises stress;
σ_0—SMYS;
$\sigma_{rel_allow_OV}$—allowable overbend relative stress.

The objective function that minimizes maximum overbend strain is

$$o_3(X) = \frac{\varepsilon_{max_OV}(X)}{\varepsilon_{allow_OV}}, \tag{17}$$

where

ε_{max_OV}—maximum overbend strain;
ε_{allow_OV}—allowable overbend strain.

The objective function that minimizes the maximum sagbend bending moment is

$$o_4(X) = \frac{M_{b_max_SAG}(X)}{M_{b_allow_SAG}}, \tag{18}$$

where

$M_{b_max_SAG}$—maximum sagbend bending moment;
$M_{b_allow_SAG}$—allowable sagbend bending moment.

The objective function that minimizes maximum sagbend relative stress is

$$o_5(X) = \frac{\sigma_{rel_max_SAG}(X)}{\sigma_{rel_allow_SAG}}, \tag{19}$$

where

$\sigma_{rel_max_SAG}$—maximum sagbend relative stress defined with

$$\sigma_{rel_max_SAG}(X) = \frac{\sigma_{e_max_SAG}(X)}{\sigma_0}, \tag{20}$$

$\sigma_{e_max_SAG}$—maximum sagbend equivalent Von Mises stress;
$\sigma_{rel_allow_SAG}$—allowable sagbend relative stress.

The objective function that minimizes maximum sagbend strain is

$$o_6(X) = \frac{\varepsilon_{max_SAG}(X)}{\varepsilon_{allow_SAG}}, \tag{21}$$

where

ε_{max_SAG}—maximum sagbend strain;
ε_{allow_SAG}—allowable sagbend strain.

At least one of these criteria must be included for optimization in the overbend and one in the sagbend, and all three can be included simultaneously, resulting in a minimum of two and a maximum of six criteria. All included criteria have equal importance in either the overbend or sagbend, so they have equal weight factors. Since maximum loads typically occur at the pipe support location in the model, the distribution of weight factors between overbend and sagbend regions depends on the relative number of supports in each region. Additionally, an FT objective weight scaling factor is introduced to prioritize tensioner force minimization over other objectives when all constraints are met. The following general expression for objective function weighting factors addresses these optimization requirements for defined overbend objectives (criteria):

$$ow_i = oa_i \cdot FT \cdot 0.7 \cdot \frac{N_{S_OV} + 1}{N_S + 1} \cdot \frac{1}{\sum_{k=1}^{N_{CRIT_OV}} oa_k}, \; i \in \{1, \ldots, N_{CRIT_OV}\} \tag{22}$$

and for defined sagbend objectives,

$$ow_j = oa_j \cdot FT \cdot 0.7 \cdot \frac{N_{S_SAG}}{N_S + 1} \cdot \frac{1}{\sum_{k=N_{CRIT_OV}+1}^{N_{CRIT}} oa_k}, \; j \in \{N_{CRIT_OV} + 1, \ldots, N_{CRIT}\} \tag{23}$$

where

N_{S_OV}—number of supports in overbend area;
N_{S_SAG}—number of supports in sagbend area;
$N_S = N_{S_OV} + N_{S_SAG}$—total number of supports;
$N_{CRIT_OV} = 3$—number of overbend objectives (criteria);
$N_{CRIT_SAG} = 3$—number of sagbend objectives (criteria);
$N_{CRIT} = N_{CRIT_OV} + N_{CRIT_SAG} = 6$—total number of objectives (criteria) in the overbend and sagbend;
oa_i—involvement (activity) of objective (criteria) in the overbend and sagbend (0—inactive | 1—active);

FT = 0.1—objectives' weight scaling factor compared to the tensioner force minimization priority.

A scaling factor of 0.7 is applied to the overall fitness function value when all weighted objective functions are summed together. A scaling factor of 0.2 is applied for the weighting factor of the objective function that minimizes the deviation of the criteria on the supports (Equation (26)), and a scaling factor of 0.1 is used for the weighting factor of the objective function that minimizes the cumulative distance of the supports from the pipe (Equation (28)).

The objective of minimizing the deviation of criteria on supports aims to equalize loads on individual supports and achieve a uniform load distribution. The standard deviation $\sigma_{STD_\sigma_rel}$ of relative stress on all supports in the overbend and sagbend is calculated using

$$\sigma_{STD_\sigma_rel} = \frac{1}{N_S} \frac{\sum_{i=1}^{N_S} (\sigma_{rel,i} - \overline{\sigma}_{rel})^2}{\overline{\sigma}_{rel}^2(X)} \tag{24}$$

The objective function that minimizes the deviation of the criteria on the supports is scaled to the interval [0,1] using the arctan function

$$o_7(X) = \frac{2}{\pi} arctan(10 \cdot \sigma_{STD_\sigma_rel}), \tag{25}$$

The corresponding weighting factor is calculated based on the previously defined objectives' weight scaling factor compared to the tensioner force minimization priority FT.

$$ow_7 = 0.2 \cdot FT. \tag{26}$$

Minimizing the cumulative distance of the supports from the pipe aims to bring non-contacting supports closer to the pipe and achieve a configuration where all supports are in contact and have positive reaction forces. That is achieved using the following objective function:

$$o_8(X) = \sum_{i=1}^{N_S} d_i(X) \tag{27}$$

where d_i is the distance of the i-th support from the pipe and the corresponding weighting factor is calculated based on the previously defined objective weight scaling factor and the tensioner force minimization priority FT.

$$ow_8 = 0.1 \cdot FT. \tag{28}$$

The primary goal of tensioner force optimization is to apply the minimum necessary force while ensuring that all constraints are met. Initially, the primary focus is to achieve a configuration that satisfies all constraints, regardless of the tensioner force magnitude. Once all constraints are satisfied, the tensioner force minimization becomes the highest priority. When all constraints are satisfied, the quality function takes a value of $f(x) < 1$, and the absolute quality function takes a value of $F(x) > 1$.

The objective function and weighting factor defined as follows achieve this goal:

$$o_9(X) = \frac{T}{T_{max}}, \tag{29}$$

$$ow_9 = \begin{cases} 0 & for \quad f(X) > 1 \\ 0.9 & for \quad f(X) \leq 1 \end{cases}. \tag{30}$$

3.4. Penalty Functions

The penalty function method is widely used to transform constrained optimization problems into unconstrained problems suitable for genetic algorithm optimization [73].

A cost or penalty is associated with the fitness function evaluation for each constraint violation. The penalty function for constraint violation has the following general form:

$$P(X) = \sum_{j=1}^{NC} cw_j \cdot p_j(X), \tag{31}$$

where NC represents the number of constraints. Each component of the penalty function is typically defined as a linear function with a penalty jump:

$$p_j(X) = \begin{cases} 0 & for \quad C_{\max}(X) \le C_{allow} \\ PJ_j + \frac{C_{\max}(X)}{C_{allow}} & for \quad C_{\max}(X) > C_{allow} \end{cases}, \tag{32}$$

where

cw_j—the constraint component weighting factor. In this implementation, for all constraints, it is set to one: $cw_j = 1$, $j \in \{1, \ldots, \mathrm{NC}\}$;
PJ_j—the penalty jump for a specific constraint. In this implementation, for all constraints, it is set to one: $PJ_j = 1$, $j \in \{1, \ldots, \mathrm{NC}\}$;
$C_{max}(X)$—the maximum value of an arbitrary criterion within the observed region;
C_{allow}—the allowable value of an arbitrary criterion within the observed region.

The penalty function for exceeding the allowable overbend bending moment is

$$p_1(X) = \begin{cases} 0 & for \quad M_{b_max_OV}(X) \le M_{b_allow_OV} \\ 1 + \frac{M_{b_max_OV}(X)}{M_{b_allow_OV}} & for \quad M_{b_max_OV}(X) > M_{b_allow_OV} \end{cases}. \tag{33}$$

The penalty function for exceeding the allowable overbend relative stress is

$$p_2(X) = \begin{cases} 0 & for \quad \sigma_{rel_max_OV}(X) \le \sigma_{rel_allow_OV} \\ 1 + \frac{\sigma_{rel_max_OV}(X)}{\sigma_{rel_allow_OV}} & for \quad \sigma_{rel_max_OV}(X) > \sigma_{rel_allow_OV} \end{cases}. \tag{34}$$

The penalty function for exceeding the allowable overbend strain is

$$p_3(X) = \begin{cases} 0 & for \quad \varepsilon_{max_OV}(X) \le \varepsilon_{allow_OV} \\ 1 + \frac{\varepsilon_{max_OV}(X)}{\varepsilon_{allow_OV}} & for \quad \varepsilon_{max_OV}(X) > \varepsilon_{allow_OV} \end{cases}. \tag{35}$$

The penalty function for exceeding the allowable sagbend bending moment is

$$p_4(X) = \begin{cases} 0 & for \quad M_{b_max_SAG}(X) \le M_{b_allow_SAG} \\ 1 + \frac{M_{b_max_SAG}(X)}{M_{b_allow_SAG}} & for \quad M_{b_max_SAG}(X) > M_{b_allow_SAG} \end{cases}. \tag{36}$$

The penalty function for exceeding the allowable sagbend relative stress is

$$p_5(X) = \begin{cases} 0 & for \quad \sigma_{rel_max_SAG}(X) \le \sigma_{rel_allow_SAG} \\ 1 + \frac{\sigma_{rel_max_SAG}(X)}{\sigma_{rel_allow_SAG}} & for \quad \sigma_{rel_max_SAG}(X) > \sigma_{rel_allow_SAG} \end{cases} \tag{37}$$

The penalty function for exceeding the allowable sagbend strain is

$$p_6(X) = \begin{cases} 0 & for \quad \varepsilon_{max_OV}(X) \le \varepsilon_{allow_OV} \\ 1 + \frac{\varepsilon_{max_OV}(X)}{\varepsilon_{allow_OV}} & for \quad \varepsilon_{max_OV}(X) > \varepsilon_{allow_OV} \end{cases} \tag{38}$$

The number of penalty functions for exceeding allowable support reactions is equal to the total number of supports, N_S. Each support can have a unique allowable reaction force.

$$p_i(X) = \begin{cases} 0 & za \quad R_i(X) \le R_{allow,i} \\ 1 + \frac{R_i(X)}{R_{allow,i}} & za \quad R_i(X) > R_{allow,i} \end{cases}, i \in \{N_{CRIT} + 1, \ldots, N_{CRIT} + N_S\}, \tag{39}$$

where

$R_i(X)$—reaction force on the i-th support;
$R_{allow,i}$—allowable reaction force on the i-th support.

3.5. Crossover

Due to the variability in optimized variable types, a flexible crossover procedure is selected as the most appropriate approach. The developed flexible crossover procedure combines the following standard basic crossover operators:

- Uniform crossover;
- One-point crossover;
- Average crossover.

Each basic crossover operator has a corresponding probability assigned to it. This probability determines the likelihood of the individual operator being activated when a crossover operation takes place. These three individual probabilities sum up to one. The total crossover probability defines the likelihood of a crossover operation occurring at all.

3.6. Mutation

A complex mutation operator application procedure has been developed to adapt GA behavior to the specific requirements of installation configuration optimization, ultimately achieving maximum optimization efficiency. In addition to the standard general mutation operators (strong and weak mutation), special mutation operators tailored to the specific S-Lay installation method configuration optimization problem have been developed. These operators are grounded in the geometry and physics of the S-Lay method model. Each mutation operator from the following list has a corresponding mutation operator probability assigned. Similar to the crossover operator probabilities, each mutation operator probability determines the likelihood of activating the particular operator when mutation operation takes place. Moreover, these individual probabilities sum up to one. The total mutation probability determines the likelihood of mutation occurring. The following is a list of developed mutation operators with their descriptions:

- Strong mutation—each gene can randomly change its value within the entire range of the associated optimization variable. This corresponds to the standard GA mutation operator;
- Weak mutation—each gene can randomly change its value, but only to the nearest integer value of the associated optimization variable. This type of mutation operator is well suited for shape optimization problems and should have a significantly higher probability of being applied compared to the strong mutation operator;
- Support-to-pipe mutation—this mutation simultaneously modifies multiple genes associated with supports' heights, raising each support until it touches the pipe if there is a gap between them. The gap between the support and the pipe is calculated based on their vertical distance and the corresponding support height is increased to close the gap or to the maximum allowable support height if necessary;
- Stinger angle mutation—this mutation combines a change in the stinger angle with adjustments to the supports, similar to the support-to-pipe mutation operator. Since a small change in the stinger angle can affect the contact of the stinger rollers with the pipe, it is necessary to correct the rollers' positions to maintain proper configuration and contact with the pipe without overstressing the pipe due to excessive support heights;
- Reaction-based support mutation—this mutation adjusts multiple genes associated with support heights to achieve more uniform distribution of support reactions. It compares the reactions at all vessel or stinger supports, lowering the heights of supports with higher reactions and raising the heights of supports with lower reactions than the average. The magnitude of the adjustments is proportional to the deviation of the corresponding supports' reactions from the average value;

- Tension mutation—due to the inherent geometry of S-Lay installation configuration, small changes in tensioner force can significantly impact bending loads and support reactions. This can lead to infeasible configurations and fitness functions' drops due to the constraint violation if tensioner force is adjusted without corresponding adjustments to support heights. The tension mutation operator addresses this issue by simultaneously altering tensioner force and supports' heights. When tensioner force is increased, the heights of more distant vessel and stinger supports are proportionally increased in order to maintain a consistent radius of curvature and vice versa;
- Bending moment-based support mutation—this operator is similar to the reaction-based support mutation operator. Multiple genes associated with support heights are adjusted to achieve a more uniform distribution of bending moments at pipe nodes located above supports;
- Extreme support mutation—this operator corrects the heights of supports that have extreme values of constraint functions. The support height is adjusted toward the heights of its two neighboring supports.

4. Results and Discussion

The developed multi-objective genetic algorithm was applied and tested on two distinctive and representative test cases:

1. A 32-inch outer diameter (OD) pipeline with concrete weight coating (CWC) installation at a moderate water depth of 50 m;
2. A 16-inch pipeline without CWC installation at a higher water depth of 400 m.

Both test cases adhere to prescribed mixed pipe integrity criteria based on the DNVGL-ST-F101 standard [65]. In the overbend region, the DCC-combined loading criterion with its defined limiting total strain was applied, while in the sagbend region, the LCC-combined loading criterion with its defined limiting bending moment was applied. Both test cases utilize the same pipelay vessel and stinger (Section 4.1) and employ the same GA optimization parameters (Section 4.2).

Due to the stochastic nature of GA optimization, each optimization run on the same test case will exhibit a unique course but should converge to optimal values for the main optimized parameters—the tensioner force, maximum bending moment and strain. A key characteristic of S-Lay installation configuration optimization is that there exist multiple combinations of the support heights, stinger angle and pipelay vessel trim and draft that can produce the same pipe string geometry and installation loads for the same tensioner force. To assess the effectiveness of the developed GA, both test case optimizations were conducted five times and primary optimization results are presented for each run, along with the mean value of the observed optimization parameter. The best optimal configurations are chosen and presented based on the maximum fitness function value achieved across all optimization runs.

4.1. Test Pipelay Vessel and Stinger

Tables 1–3 summarize the pipelay vessel and stinger geometry employed for both test cases involving an S-Lay method installation configuration analysis and optimization. The pipelay vessel incorporates four adjustable deck supports and is equipped with a rigid stinger of an approximate length of 50 m with five adjustable supports.

Table 1. Test pipelay vessel and stinger parameters.

Name	Symbol	Unit	Min. Value	Max. Value
Vessel draft	D_v	m	4.0	8.0
Vessel trim	ϕ_v	°	−1.8	0.0
Tensioner force	T	tf/kN	10/98.1	150/1471.5
Stinger angle	φ_s	°	0.0	90.0

Table 2. Test pipelay vessel geometry data in vessel coordinate system (x_v, z_v).

Symbol	x_v	z_{v_min}	z_{v_max}	R_{allow}
Unit	**m**	**M**	**m**	**tf/kN**
Tensioner	44.0	8.0	NA	80/784.8
Support VR1	34.0	5.0	7.0	80/784.8
Support VR2	24.0	4.0	6.0	80/784.8
Support VR3	14.0	2.0	4.0	80/784.8
Support VR4	4.0	1.0	2.0	80/784.8
Stinger hinge	−1.0	−2.0	NA	NA

Table 3. Test stinger geometry data in stinger coordinate system (x_s, z_s).

Symbol	x_s	z_{s_min}	z_{s_max}	R_{allow}
Unit	**m**	**M**	**m**	**tf/kN**
Stinger hinge	0.0	0.0	NA	NA
Support SR1	7.0	1.0	4.0	80/784.8
Support SR2	17.0	2.0	5.0	80/784.8
Support SR3	27.0	1.5	5.5	80/784.8
Support SR4	37.0	2.0	5.0	80/784.8
Support SR5	47.0	1.0	4.0	80/784.8

4.2. GA optimization Parameters

The configuration optimization problem involves thirteen optimization variables: the tensioner force, vessel trim, draft, four adjustable vessel supports, five adjustable stinger supports and stinger angle. Table 4 presents the range values and applied integer discretization step for the integer GA optimization variables.

Table 4. Test case 1 integer GA configuration optimization variables' settings.

Name	Unit	Min. Value	Max. Value	Discretization Step
Tensioner force	tf	10	150	5
Vessel draft	m	4.0	8.0	0.01
Vessel trim	°	−1.8	0.0	0.1
Vessel supports' heights	m	NA [1]	NA [1]	0.001
Stinger supports' heights	m	NA [2]	NA [2]	0.001
Stinger angle	°	0.0	90.0	0.001

[1] See Table 2. [2] See Table 3.

Table 5 summarizes the GA settings and operator probabilities employed for test case configuration optimization. Five GA optimization runs were executed, each with a fixed number of generations set to 200.

The total crossover probability was set to 0.75, while probabilities for each basic crossover operator were nearly equal, with a slightly higher probability of 0.4 assigned to the average crossover.

The total mutation probability was set to 0.65. The highest individual mutation operator probability of 0.4 was assigned to weak mutation, while the lowest probability of 0.01 was assigned to strong mutation. This was carried out to ensure a relatively low occurrence of standard mutation across the entire range of optimized variable values (strong mutation) while maintaining a higher number of random, small changes in optimization variables due to the nature of the optimization problem. The remaining probabilities were distributed almost equally among the other specialized mutation operators, with support-to-pipe mutation and tension mutation receiving half the remaining probabilities to keep them suppressed relative to other operators. The sum of all individual operator probabilities should equal to one.

Table 5. GA optimization parameters.

Parameter	Value
Population size	56
Number of generations	200
Tournament selection size	6
Tournament selection 1st chromosome probability	0.2
Tournament selection 2nd chromosome probability	0.4
Roulette wheel 1st chromosome probability	0.8
Roulette wheel 2nd chromosome probability	0.6
Total crossover probability	0.75
Uniform crossover probability	0.3
One-point crossover probability	0.3
Average crossover probability	0.4
Total mutation probability	0.65
Strong mutation probability	0.01
Weak mutation probability	0.400
Support-to-pipe mutation probability	0.059
Stinger angle mutation probability	0.118
Mutation via supports' reaction probability	0.118
Tension mutation probability	0.059
Supports' mutation via bending moment probability	0.118
Mutation of extreme supports' probability	0.118

Both test cases employ the same two installation analysis criteria, as defined in [60]. The allowable overbend strain limit triggers objective function Equation (17) and penalty function Equation (35). Similarly, the allowable sagbend bending moment activates objective function Equation (18) and penalty function Equation (36). Additionally, GA optimization utilizes objective function Equation (25) to minimize the deviation of the criteria at supports and objective function Equation (27) to minimize the cumulative distance between supports and the pipe. Finally, due to the tensioner force optimization, objective function Equation (29) for tensioner force minimization is employed. In total, this yields five objectives for the GA multi-objective optimization process.

Other installation criteria objectives and penalty functions described in Sections 3.2 and 3.3 are inactive (not employed). Table 6 presents five objective function weight factors applied for the GA optimization, calculated in accordance with the corresponding equations provided in Section 3.2. The sum of active objective function weight factors equals one, as per Equation (13).

Table 6. Active objective function weight factors used in GA optimization.

Parameter	Weight Factor	Value
Maximum overbend strain	ow_3	0.0573
Maximum sagbend bending moment	ow_4	0.0127
Deviation of the criteria on the supports	ow_7	0.0200
Cumulative distance of the supports from pipe	ow_8	0.0100
Tensioner force	ow_9	0.9000

4.3. Test Case 1

Test case 1 involves S-Lay installation of a 32 inch (812.8 mm)-diameter pipeline with a wall thickness of 22.2 mm at a water depth of 50 m. The pipe steel grade is X65 with an SMYS of 450 MPa. To ensure pipeline on-bottom stability, the pipe is coated with a 50-mm-thick concrete weight coating. The concrete weight coating does not affect the pipe steel integrity criteria but does increase the overall pipe weight. The allowable overbend strain limit is set to 0.2%, following the concrete coating crushing limiting pipe strain criterion. The allowable sagbend bending moment is calculated according to the DNV-ST-F101 [65]

LCC-combined loading criterion, assuming a 30% increase in the static bending moment due to environmental loads (the dynamic bending moment component is assumed to be 30% of the static bending moment). The pipeline parameters and pipelay static analysis criteria for test case 1 are summarized in Table 7.

Table 7. Test case 1 pipeline parameters and pipelay static analysis criteria.

Name	Symbol	Unit	Value
Water depth	WD	m	50
Outside pipe diameter	OD	"/m	32/812.8
Pipe wall thickness	t_w	mm	22.2
Pipe steel density	ρ_s	kg/m^3	7850
Pipe steel modulus of elasticity	E_s	GPa	210
Concrete coating thickness	t_c	mm	50
Concrete coating density	ρ_c	kg/m^3	3050
Concrete coating modulus of elasticity	E_c	GPa	33
Pipe weight in air [1]	w	kg/m	882
Submerged pipe weight [1]	w_s	kg/m	188
Specified minimum yield strength	$SMYS$	MPa	450
Allowable overbend strain	ε_{allow_OV}	%	0.2
Allowable sagbend bending moment	$M_{b_allow_OV}$	kNm	3433.5

[1] Including concrete weight coating.

Figure 6 depicts the evolution of the best individual fitness function value across five GA optimization runs, alongside the mean fitness function value for all runs.

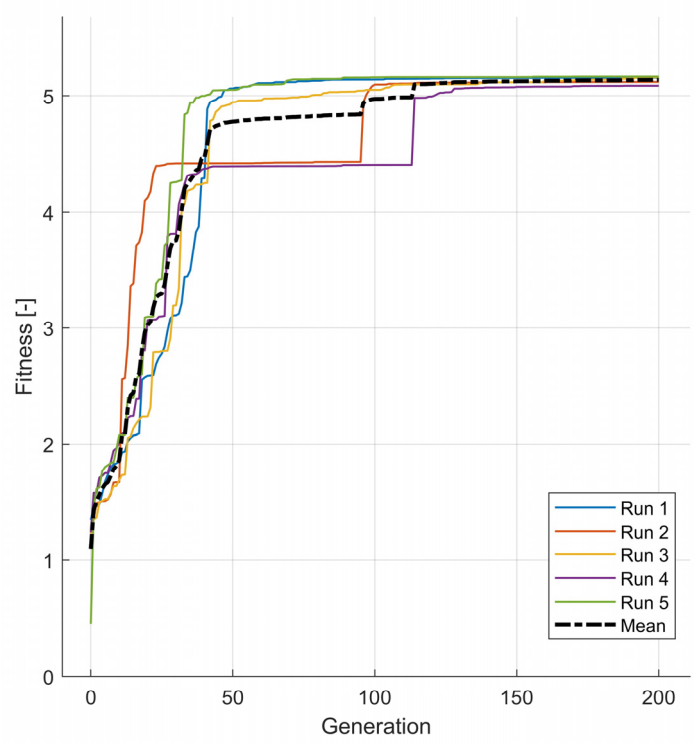


Figure 6. Test case 1: Evolution of the best individual fitness function during GA optimization.

Figure 7 offers insights into the changes in the best individual tensioner force value throughout the GA optimization runs. Figures 8 and 9 showcase the variations in the best individual objective functions corresponding to the combined loading criteria in the sagbend and overbend during the optimization runs. The evolution of the best individual cumulative distance of supports from the pipe objective function across five GA optimizations is presented in Figure 10.

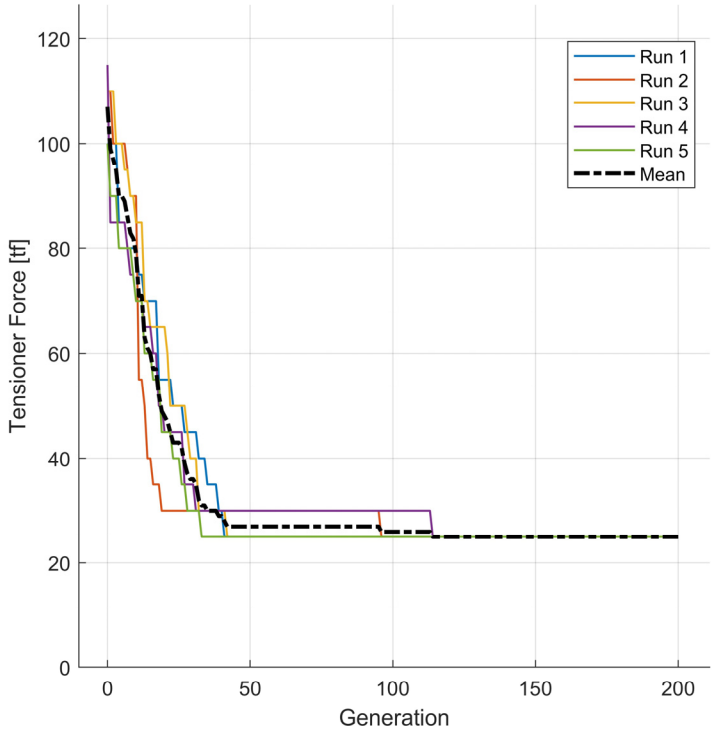


Figure 7. Test case 1: Evolution of the best individual tensioner force during GA optimization.

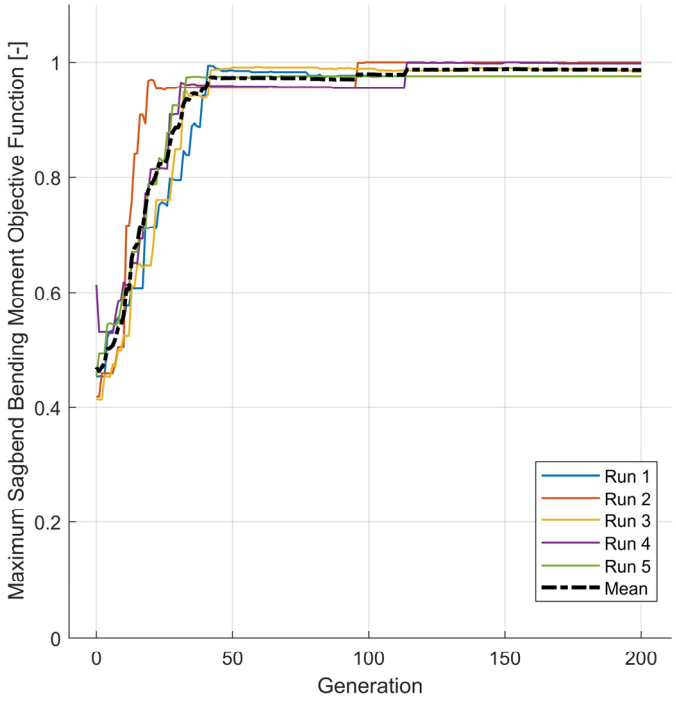


Figure 8. Test case 1: Evolution of the best individual maximum sagbend bending moment objective function (Equation (18)) during GA optimization.

The first GA optimization run yielded the optimal solution (final best individual) configuration, achieving the highest value of the fitness function. Optimized parameters are presented in Table 8. The pipe S-curve geometry and corresponding bending moment, total strain and support reaction distributions for the optimal solution are depicted in Figures 11–14, respectively. The positions of vessel and stinger supports are indicated by red dots and labels.

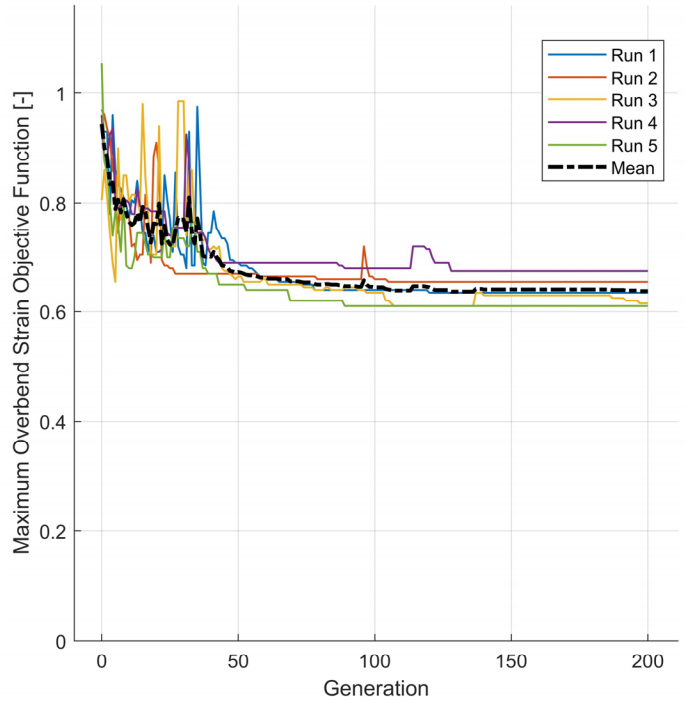


Figure 9. Test case 1: Evolution of the best individual maximum overbend strain objective function (Equation (17)) during GA optimization.

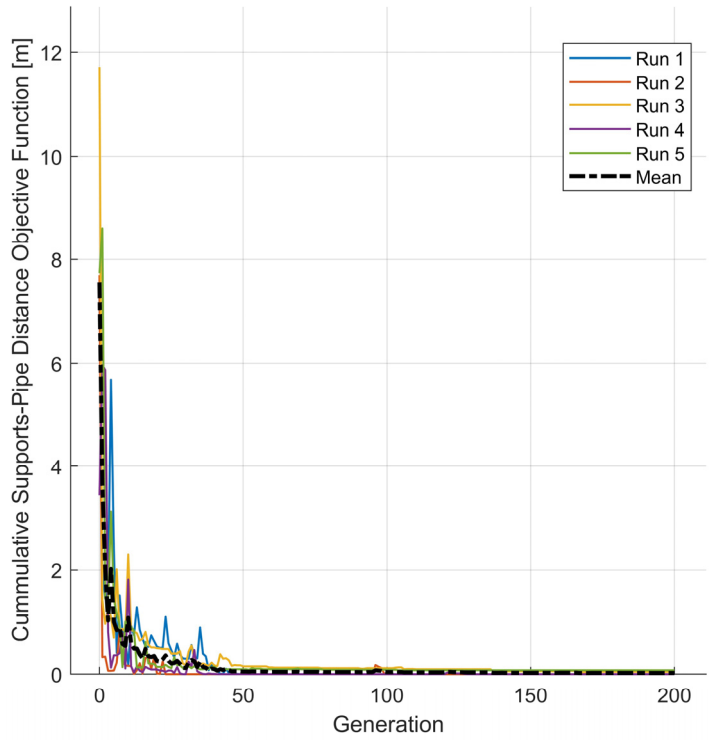


Figure 10. Test case 1: Evolution of the best individual cumulative distance of supports from pipe objective function (Equation (27)) during GA optimization.

4.4. Test Case 2

Test case 2 involves a distinctive example of S-Lay installation of a pipeline with an outer diameter of 16 inches (406.4 mm) and a wall thickness of 25.4 mm, carried out at a water depth of 400 m. The pipe steel grade is X65 with an SMYS of 450 MPa. The allowable overbend strain limit is set to 0.3%, in accordance with the DNV-ST-F101 guidelines [65].

The allowable sagbend bending moment is calculated based on the DNV-ST-F101 [65] LCC-combined loading criterion, assuming a 30% increase in the static bending moment due to environmental loads (the dynamic bending moment component is assumed to be 30% of the static bending moment). The pipeline parameters and pipelay static analysis criteria for test case 2 are summarized in Table 9.

Table 8. Test case 1 optimal solution configuration parameters.

Name	Symbol	Unit	Value
Tensioner force	T	tf/kN	25/245.25
Vessel draft	D_v	m	9.550
Vessel trim	ϕ_v	°	−0.8
Stinger angle	φ_s	°	15.865
Support VR1 height	z_{VR1}	m	6.965
Support VR2 height	z_{VR2}	m	5.604
Support VR3 height	z_{VR3}	m	3.922
Support VR4 height	z_{VR4}	m	1.918
Support SR1 height	z_{SR1}	m	2.944
Support SR2 height	z_{SR2}	m	3.010
Support SR3 height	z_{SR3}	m	2.760
Support SR4 height	z_{SR4}	m	2.199
Support SR5 height	z_{SR5}	m	1.340

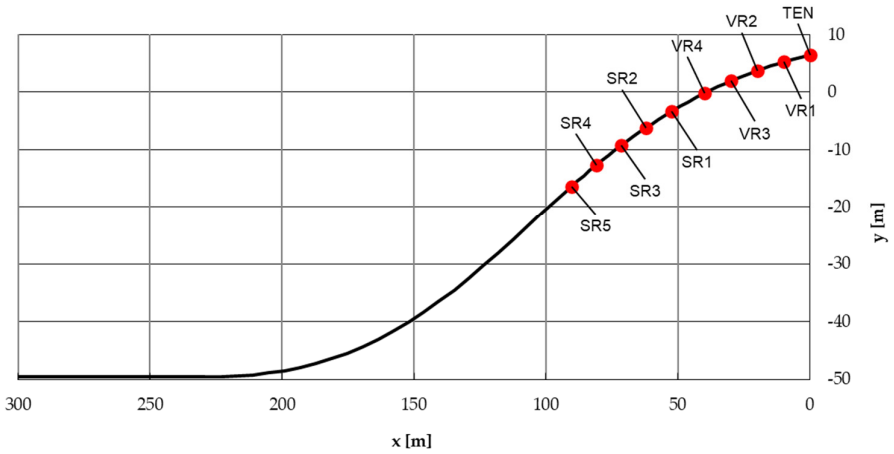


Figure 11. Test case 1 optimal solution pipe S-curve geometry.

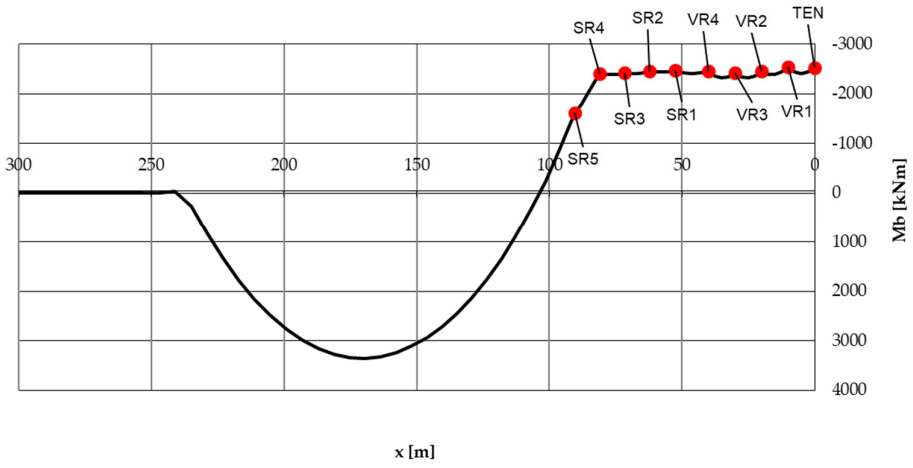


Figure 12. Test case 1 optimal solution bending moment distribution.

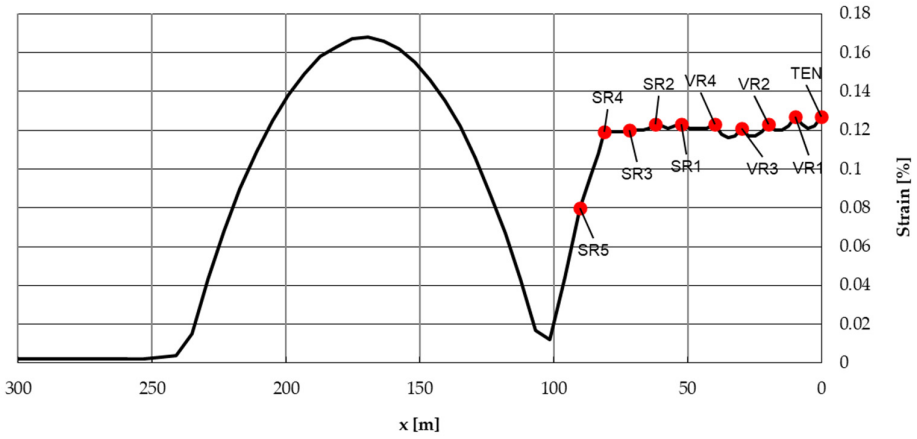


Figure 13. Test case 1 optimal solution total strain distribution.

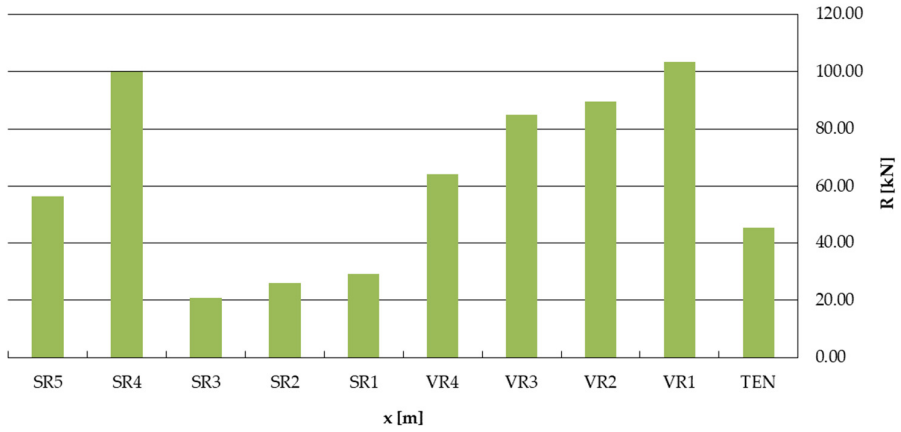


Figure 14. Test case 1 optimal solution support reactions.

Table 9. Test case 2 pipeline parameters and pipelay static analysis criteria.

Name	Symbol	Unit	Value
Water depth	*WD*	M	400
Outside pipe diameter	*OD*	“/m	14/406.4
Pipe wall thickness	t_w	Mm	25.4
Pipe steel density	ρ_s	kg/m^3	7850
Pipe steel modulus of elasticity	E_s	GPa	210
Pipe weight in air	w	kg/m	243
Submerged pipe weight	w_s	kg/m	108
Specified minimum yield strength	*SMYS*	MPa	450
Allowable overbend strain	ε_{allow_OV}	%	0.3
Allowable sagbend bending moment	$M_{b_allow_OV}$	kNm	1111.0

Figure 15 illustrates the evolution of the best individual fitness function value across five GA optimization runs, alongside the mean fitness function value for all runs.

The best individual tensioner force value alterations during GA optimizations are depicted in Figure 16. Figures 17 and 18 showcase the variations in the best individual objective functions corresponding to the combined loading criteria in the sagbend and overbend during the optimization runs. Figure 19 presents the evolution of the best individual cumulative distance of supports from the pipe objective function across five GA optimizations for test case 2.

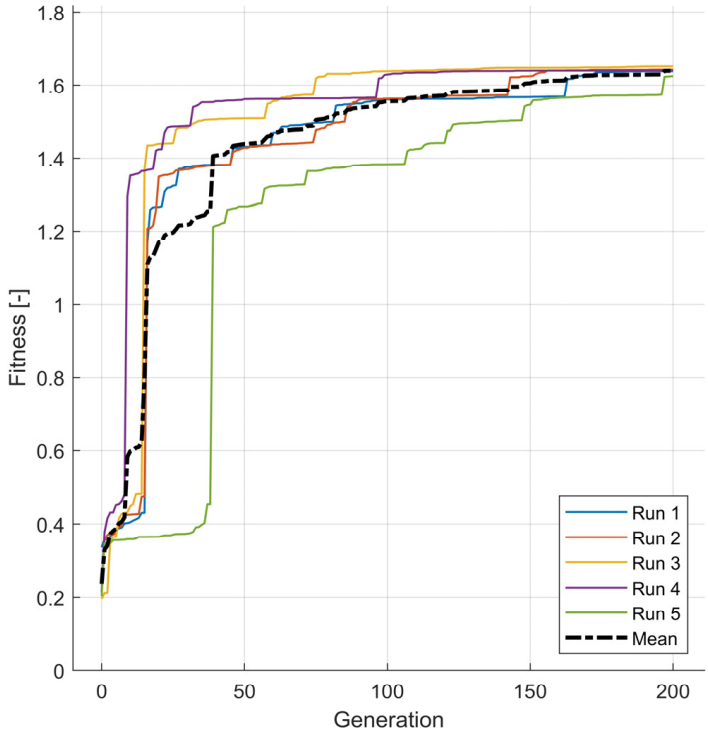


Figure 15. Test case 2: Evolution of the best individual fitness function during GA optimization.

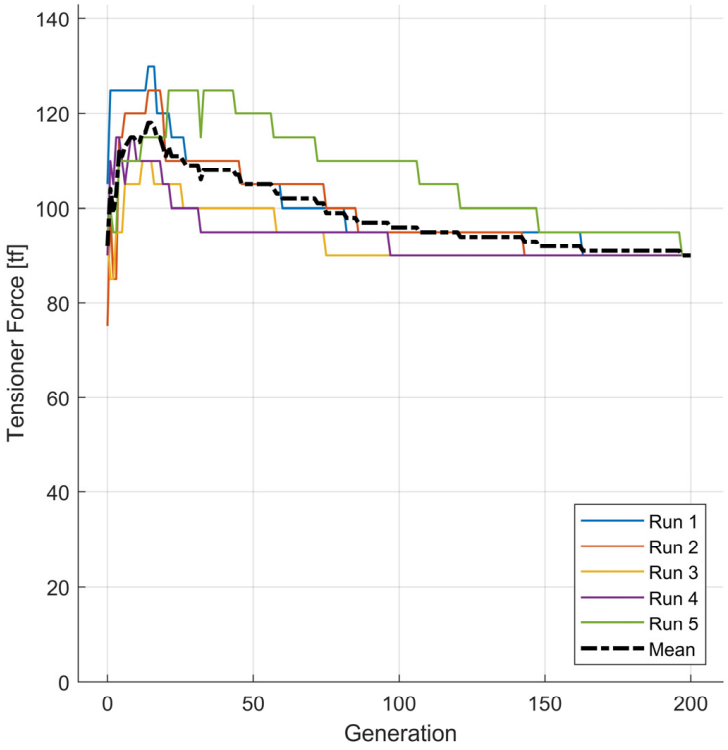


Figure 16. Test case 2: Evolution of the best individual tensioner force during GA optimization.

The third GA optimization run yielded the optimal solution (final best individual) configuration, achieving the highest value of the fitness function. Corresponding optimal solution (final best individual) configuration parameters are presented in Table 10. The pipe S-curve geometry and corresponding bending moment, total strain and support reaction distributions for the optimal solution are depicted in Figures 20–23, respectively. The

positions of vessel and stinger supports are indicated with red dots, while the first and last supports on the vessel and stinger are labeled.

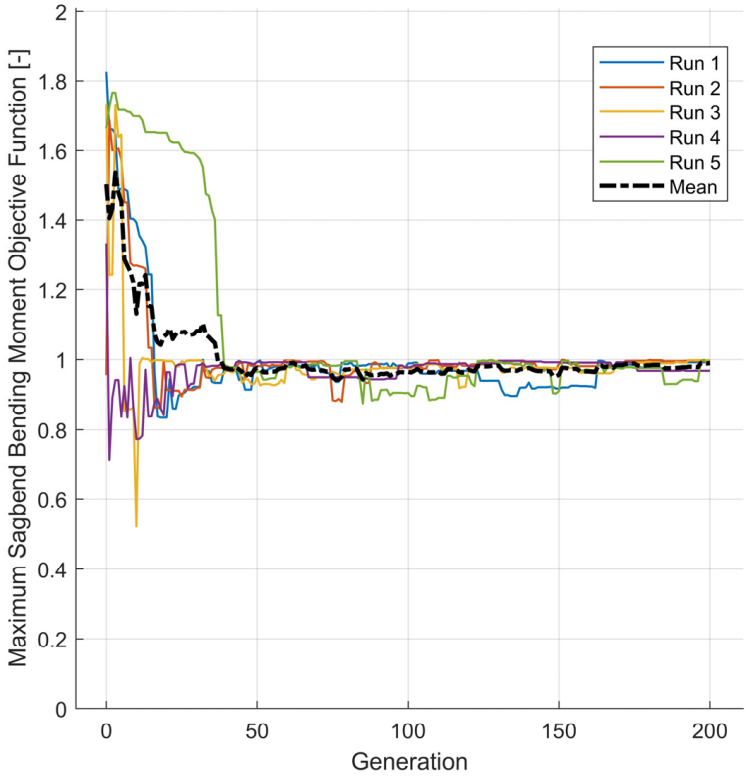


Figure 17. Test case 2: Evolution of the best individual maximum sagbend bending moment objective function (Equation (18)) during GA optimization.

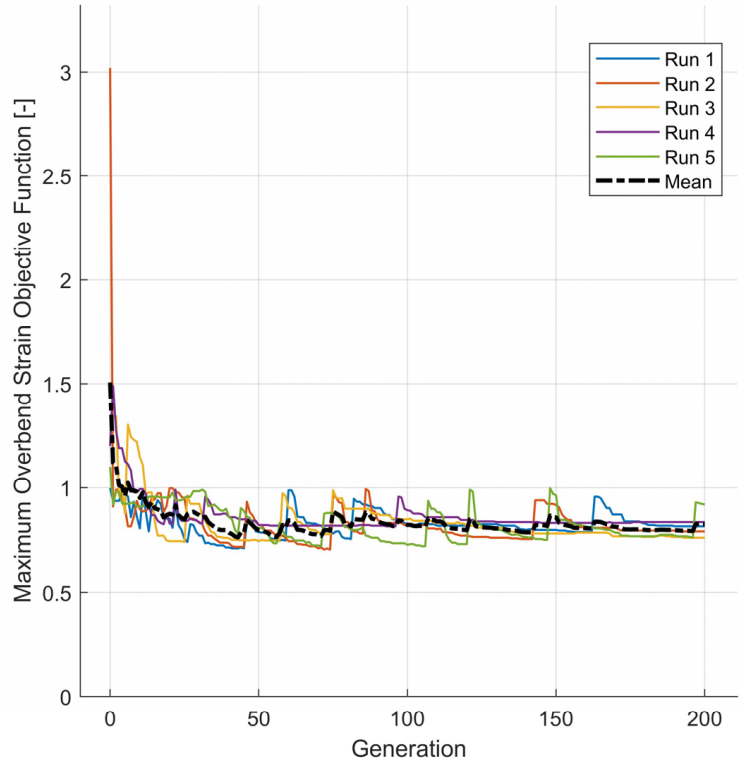


Figure 18. Test case 2: Evolution of the best individual maximum overbend strain objective function (Equation (17)) during GA optimization.

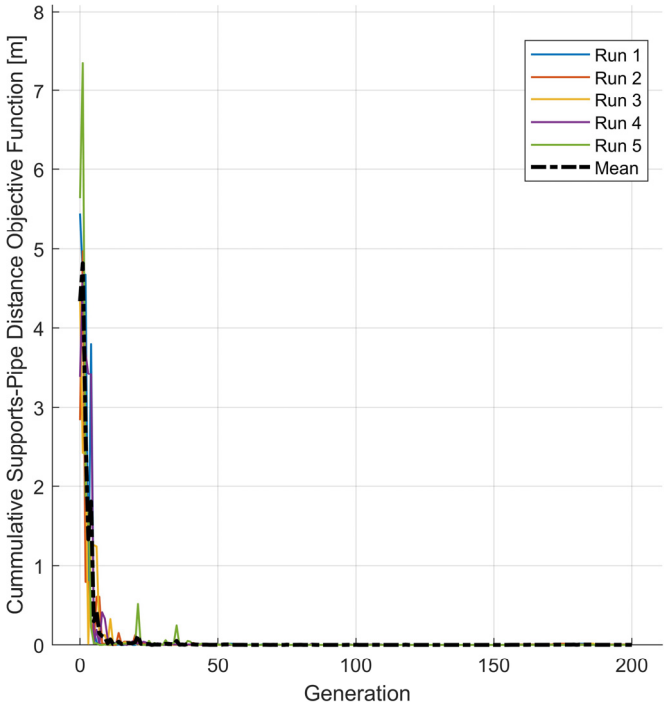


Figure 19. Test case 2: Evolution of the best individual cumulative distance of supports from pipe objective function (Equation (27)) during GA optimization.

Table 10. Test case 2 optimal solution configuration parameters.

Name	Symbol	Unit	Value
Tensioner force	T	tf/kN	90/882.9
Vessel draft	D_v	m	7.470
Vessel trim	ϕ_v	°	−1.7
Stinger angle	φ_s	°	36.977
Support VR1 height	z_{VR1}	m	6.961
Support VR2 height	z_{VR2}	m	5.602
Support VR3 height	z_{VR3}	m	3.705
Support VR4 height	z_{VR4}	m	1.000
Support SR1 height	z_{SR1}	m	2.879
Support SR2 height	z_{SR2}	m	4.366
Support SR3 height	z_{SR3}	m	4.795
Support SR4 height	z_{SR4}	m	4.177
Support SR5 height	z_{SR5}	m	2.512

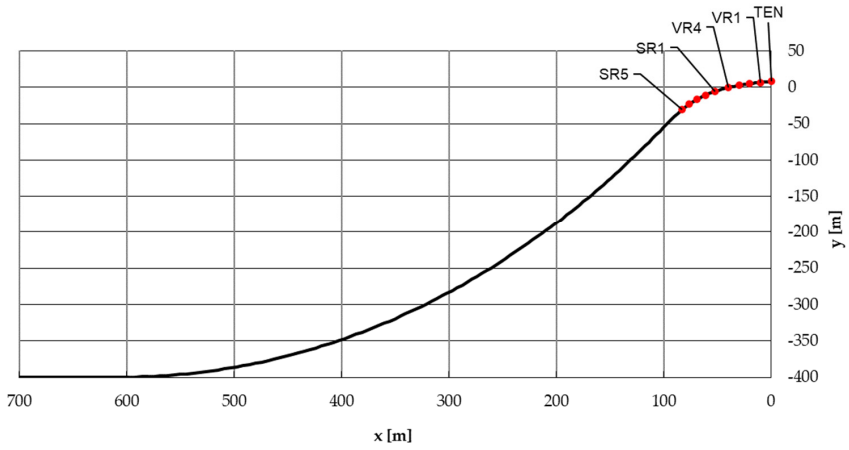


Figure 20. Test case 2 optimal solution pipe S-curve geometry.

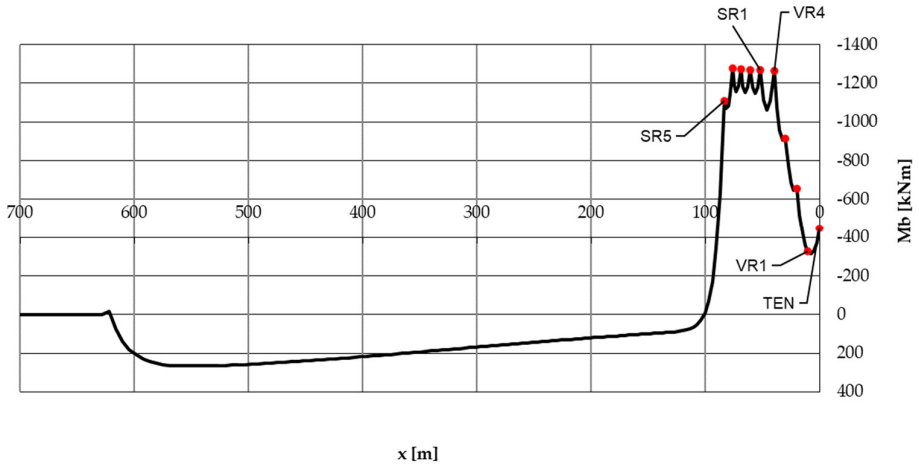


Figure 21. Test case 2 optimal solution bending moment distribution.

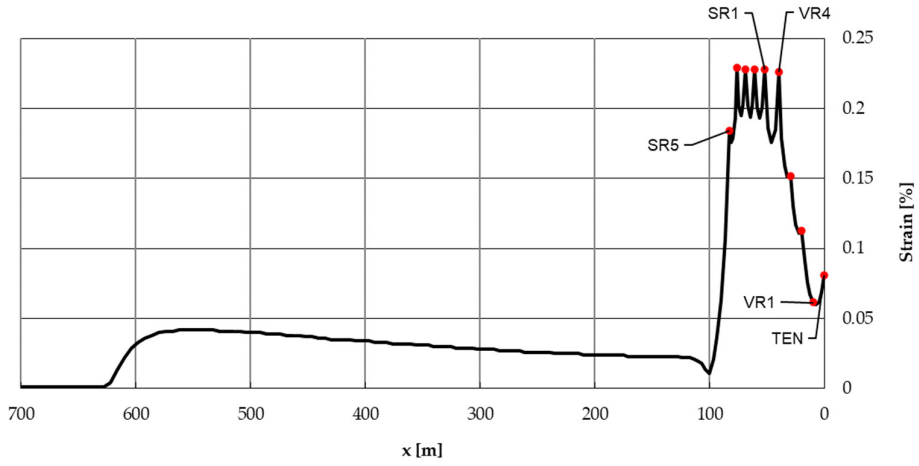


Figure 22. Test case 2 optimal solution total strain distribution.

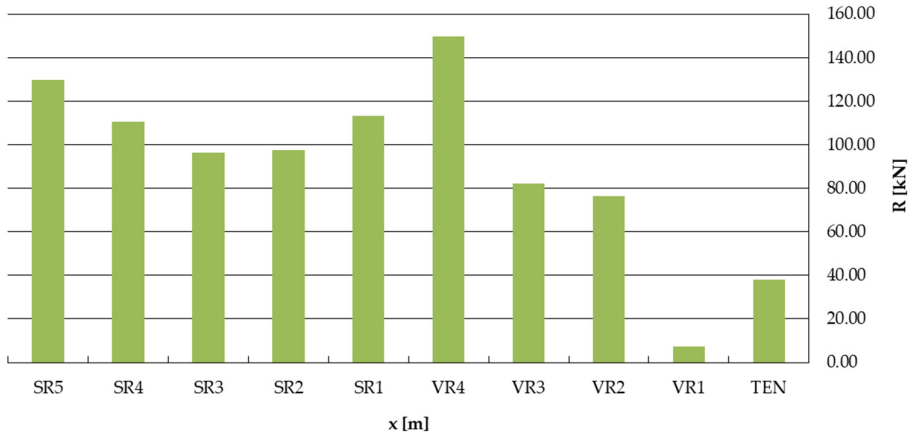


Figure 23. Test case 2 optimal solution support reactions.

4.5. Comparison with Basic Genetic Algorithm

To demonstrate the contribution and efficiency of the developed specialized mutation operators, a comparison with basic integer GA was conducted for test case 1. The basic GA configuration involved setting the probabilities of all specialized mutation operators, except the strong mutation, to zero. The strong mutation operator corresponds to the standard GA mutation operator. The strong mutation operator randomly alters every gene value

within the entire range of the corresponding optimization variable. The total mutation probability and the corresponding strong mutation probability were set to 0.65, which falls within the typical range for integer GAs. Five GA optimization runs were executed for test case 1 using the basic GA configuration. Figure 24 compares the mean fitness values across multiple runs for the developed specialized GA runs (as shown in Figure 6) with the mean fitness value during basic GA optimization for 200 generations.

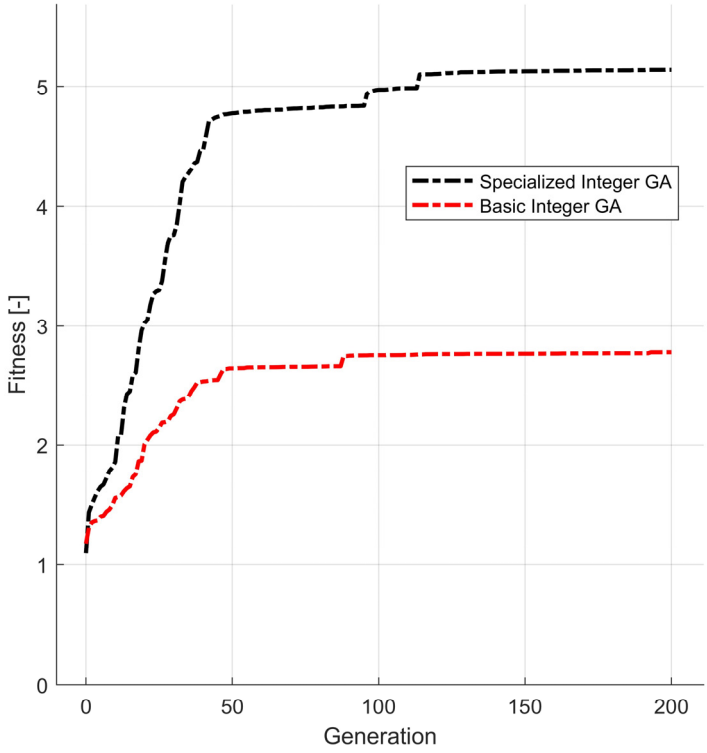


Figure 24. Test case 1 mean fitness comparison for multiple specialized and basic integer GA runs.

4.6. Discussion

Two test cases were selected to encompass the variability of two crucial parameters that define subsea pipeline installation scenarios: water depth and pipe OD. The first test case involves a higher pipe OD (32 inches) installed at a moderate water depth of 50 m. The second test case represents a 16-inch pipeline installation at an increased water depth of 400 m. The test pipelay vessel possesses a maximum tensioner capacity of 150 tf, four adjustable supports on the vessel deck and a 50-m rigid stinger with five adjustable supports attached.

Five GA optimization runs were conducted for both test cases over 200 generations. The progression of all GA optimization runs is illustrated in Figures 6 and 15. All five optimization runs for each test case successfully converged to optimal solutions with nearly identical fitness function values for the best individuals. Consequently, the key optimized parameters (tensioner force, maximum sagbend bending moment, maximum overbend strain) also converged to consistent values (Figures 7–9 and Figures 16–18). These outcomes demonstrate the efficacy and validity of the developed specialized GA. The most crucial optimized parameter, tensioner force, maintained a constant value of 25 tf for all optimization runs conducted for test case 1 (Figure 7). Figure 16 demonstrates that an optimal tensioner force of 90 tf is reached for all five optimization runs executed for test case 2.

Test case 1 GA optimization runs shown in Figure 6 demonstrate that the best individual satisfying all constraints and with a fitness value greater than 1 was obtained within the first few generations. This can be attributed to the moderate water depth of 50 m and the substantial available tensioner capacity of 150 tf, well beyond the minimum required

tension of 25 tf attained at the end of the optimization process. Figure 15 indicates that a greater number of generations is required to obtain the best individual that satisfies all constraints and surpasses a fitness value of 1 in test case 2 compared to test case 1. This is primarily due to the increased water depth, which necessitates a higher optimal tension of 90 tf for that configuration, approaching the maximum tensioner capacity.

An analysis of Figure 6 suggests that all test case 1 optimization runs attained fitness values closely approaching their final values after 125 generations, suggesting that the set number of 200 generations is excessive for this case. The optimization runs for test case 2, as depicted in Figure 15, reveal that some runs could potentially be further enhanced if the optimization process was extended for more generations, while few converged to the maximum fitness values after 100 generations. Test case 1 at a 50-m water depth presents a more straightforward optimization due to the available tensioner capacity, leading to populations saturated with higher-fitness individuals early on. However, the optimization of test case 2 at a higher water depth, requiring a greater tensioner capacity, generates populations with a substantial number of individuals that fail to meet constraints and exhibit poor fitness values. This observation underscores potential benefits of implementing a dynamic GA with adaptable mutation operator probabilities.

The evolution of optimized parameters during optimization (Figures 7–10 for test case 1 and Figures 16–19 for test case 2) demonstrates that all optimization constraints are met relatively promptly and objective functions of optimized parameters exhibit consistent improvement after constraints are satisfied.

The final optimal solutions (Figures 11–14 for test case 1 and Figures 20–23 for test case 2) conclusively demonstrate that the optimization objectives have been achieved and that the best optimal configurations fulfill all specified installation analysis goals.

A comparison with the basic integer GA is conducted for test case 1 and detailed in Section 4.4. Figure 24 clearly illustrates the superiority of the developed specialized GA over the basic GA, which employs only the strong mutation operator.

5. Conclusions

The crucial and intricate task of a subsea pipeline S-Lay method installation engineering analysis involves identifying the optimal pipelay vessel installation configuration for each distinct pipeline route section. Installation loads in the pipeline are highly sensitive to subtle alterations in the configuration of pipeline supports during pipelay, along with other influential factors like the tensioner force, stinger angle, trim and draft of the pipelay vessel. Consequently, the process of an engineering installation analysis poses a significant challenge, necessitating an automated optimization procedure.

The initial research objective focused on analyzing and systematizing the subsea pipeline installation analysis procedure. By establishing clear procedures, goals and methodology, the conditions that must be met by the optimization process were determined, leading to the formulation of the optimization problem. This optimization problem falls under the category of constrained nonlinear optimization problems involving a combination of continuous and discrete variables. Both the objective and constraint functions cannot be represented analytically but rather derive from the results of static pipelay analysis simulations. Based on these simulation outcomes, the values of individual components of the objective function are calculated and the violations of constraint functions are evaluated.

The second research objective was to develop a comprehensive optimization procedure employing a genetic algorithm that could automatically identify the optimal combination of all critical parameters governing subsea pipeline installation configuration specific to the S-Lay method. A specialized tailored multi-objective GA is designed to be adaptable to various sets of optimization criteria and offshore standards' requirements. This genetic algorithm was specifically tailored to the intricate problem of pipeline installation using the S-Lay method, ensuring compliance with all requirements established during the analysis and formulation of the S-Lay installation analysis methodology. Multi-objective constrained optimization was achieved through the implementation of a penalty function and flexible

objective and constraint prioritization via weighting factors. Tailored genetic algorithm operators specially designed for this purpose enable the efficient identification of the optimal combination of all the influential parameters governing the S-Lay installation method. This study represents the first known application of genetic algorithm optimization to the task of finding optimal subsea pipeline S-Lay method configurations. Previous research papers, as mentioned in the introduction, focused on optimizing a limited number of influential laying parameters, whereas the developed GA optimization facilitates simultaneous optimization of all influencing parameters, regardless of their number or type (continuous or discontinuous).

The developed multi-objective genetic algorithm was applied to two representative test cases. These optimized test cases were characterized by adhering to prescribed mixed pipe integrity criteria as per the DNV-ST-F101 standard [65], utilizing a pipelay vessel equipped with a single rigid stinger and a concrete-coated pipe. For the overbend region, a displacement-controlled condition with a defined limiting total strain was implemented, while for the sagbend region, a load-controlled condition with a defined limiting bending moment was employed.

Multiple GA optimization runs yielded optimal solutions that met all the optimization targets. The same minimum optimal tensioner force value was consistently obtained across all optimization runs, despite the stochastic nature of GA optimization. The efficiency of the optimization procedure and the quality of the achieved solutions demonstrate the suitability of the developed genetic algorithm operators and the overall optimization approach for the presented optimization problem and application.

Further research can proceed in several promising directions. One promising direction lies in refining the employed genetic algorithm through a more in-depth examination of the influence of specific parameters and potentially incorporating adaptative parameters (adaptive genetic algorithm) and the development of novel operators. Optimization efficiency could be enhanced by employing a hybrid genetic algorithm that utilizes a deterministic local search method toward the end of the optimization process. Another avenue involves extending the overall optimization process from single-section GA to simultaneous optimization of multiple pipeline route sections, a significantly more complex challenge.

Author Contributions: Conceptualization, D.K.; Methodology, D.K.; Software, D.K.; Validation, D.K., M.K., S.M. and L.L.; Formal analysis, D.K.; Investigation, D.K.; Resources, D.K.; Data curation, D.K.; Writing—original draft, D.K.; Writing—review and editing, D.K., M.K., S.M. and L.L. All authors have read and agreed to the published version of the manuscript.

Funding: This research received no external funding.

Institutional Review Board Statement: Not applicable.

Informed Consent Statement: Not applicable.

Data Availability Statement: The data presented in this study are available on request from the corresponding author. The data are not publicly available due to privacy.

Conflicts of Interest: The authors declare no conflicts of interest.

References

1. Zhang, H.; Feng, Q.; Yan, B.; Zheng, X.; Yang, Y.; Chen, J.; Zhang, H.; Liu, X. State of the Art of Oil and Gas Pipeline Vulnerability Assessments. *Energies* **2023**, *16*, 3439. [CrossRef]
2. Yang, Z.; Xiang, Q.; He, Y.; Peng, S.; Faber, M.H.; Zio, E.; Zuo, L.; Su, H.; Zhang, J. Resilience of Natural Gas Pipeline System: A Review and Outlook. *Energies* **2023**, *16*, 6237. [CrossRef]
3. Priasti, F.A. Resilience of HP/HT Pipelines to Combined Seismic and Thermal Loadings. *Ocean Eng.* **2023**, *275*, 114098. [CrossRef]
4. Xu, P.; Du, Z.; Gong, S. Numerical Investigation into Freak Wave Effects on Deepwater Pipeline Installation. *J. Mar. Sci. Eng.* **2020**, *8*, 119. [CrossRef]
5. Okoro, A.; Khan, F.; Ahmed, S. A Methodology for Time-varying Resilience Quantification of an Offshore Natural Gas Pipeline. *J. Pipeline Sci. Eng.* **2022**, *2*, 100054. [CrossRef]
6. Ma, J.; Chen, G.; Zeng, T.; Zhou, L.; Zhao, J.; Zhao, Y. Methodology for Resilience Assessment of Oil Pipeline Network System Exposed to Earthquake. *Sustainability* **2023**, *15*, 972. [CrossRef]

7. Daley, G.C. Optimization of Tension Level and Stinger Length for Offshore Pipeline Installation. *Offshore Technol. Conf.* **1974**, *96*, 1334–1336. [CrossRef]
8. Maier, G.; Corradi, L.; Mazzoli, A.; Michelini, R. Optimization of Stinger Geometry for Deepsea Pipelaying. *Trans. ASME* **1982**, *104*, 294–301. [CrossRef]
9. Bhavikatti, S.S.; Akram, P.; Ravichandran, T.V. Minimization of Maximum Moment in Offshore Pipeline During Installation. *Appl. Ocean Res.* **1986**, *8*, 164–168. [CrossRef]
10. Zhu, D.S.; Cheung, Y.K. Optimization of Buoyancy of an Articulated Stinger on Submerged Pipelines Laid with a Barge. *Ocean Eng.* **1997**, *24*, 301–311. [CrossRef]
11. Ivić, S.; Družeta, S.; Hreljac, I. S-lay Pipe Laying Optimization Using Specialized PSO Method. *Struct. Multidiscip. Optim.* **2017**, *56*, 301–311. [CrossRef]
12. Wang, B.P.; Chen, J.L. Application of Genetic Algorithm for the Support Location Optimization of Beams. *Comput. Struct.* **1996**, *58*, 797–800. [CrossRef]
13. Chiba, T.; Okado, S.; Fujii, I.; Itami, K.; Hara, F. Optimum Support Arrangement of Piping Systems Using Genetic Algorithm. *J. Press. Vessel. Technol.* **1996**, *118*, 507–512. [CrossRef]
14. Tabakov, P.Y. Multi-dimensional Design Optimisation of Laminated Structures Using an Improved Genetic Algorithm. *Compos. Struct.* **2001**, *54*, 349–354. [CrossRef]
15. Vieira, L.T.; Pires de Lima, B.S.L.; Evsukoff, A.G.; Jacob, B.P. *Application of Genetic Algorithms to the Synthesis of Riser Configurations*; American Society of Mechanical Engineers Digital Collection: Lawrence, KS, USA, 2003.
16. Vieira, I.N.; Silva, A.J.M.; de Lima, B.S.L.P.; Jacob, B.P. A comparative study applied to risers optimization using bio-inspired algorithms. *Intl. J. Model. Simul. Pet. Ind.* **2009**, *3*.
17. Gantovnik, V.B. An Improved Genetic Algorithm for the Optimization of Composite Structures. Ph.D. Thesis, Virginia Polytechnic Institute, Blacksburg, VA, USA, 2005.
18. Shafieefar, M.; Rezvani, A. Mooring Optimization of Floating Platforms Using a Genetic Algorithm. *Ocean Eng.* **2007**, *34*, 1413–1421. [CrossRef]
19. Boulougouris, E.; Papanikolaou, A. Multiobjective Optimisation of a Floating LNG Terminal. *Ocean Eng.* **2008**, *35*, 787–811. [CrossRef]
20. Clauss, G.F.; Birk, L. Hydrodynamic Shape Optimization of Large Offshore Structures. *Appl. Ocean Res.* **1996**, *18*, 157–171. [CrossRef]
21. Birk, L.; Clauss, G.F.; Lee, J.Y. *Practical Application of Global Optimization to the Design of Offshore Structures*; American Society of Mechanical Engineers: New York, NY, USA, 2004.
22. Lee, J.Y.; Clauss, G.F. Automated development of floating offshore structures in deepwater with verified global preformances by coupled analysis. In Proceedings of the 17th ISOPE, Lisbon, Portugal, 1–6 July 2007.
23. de Lima, M.H.A., Jr.; Baioco, J.; Albrecht, C.; Lima, B.; Jacob, B.; Rocha, D.; Cardoso, C. Synthesis and Optimization of Submarine Pipeline Routes Considering On-Bottom Stability Criteria. In Proceedings of the International Conference on Offshore Mechanics and Arctic Engineering—OMAE, Rotterdam, The Netherlands, 19–24 June 2011; pp. 307–318. [CrossRef]
24. Baioco, J.S.; Stape, P.; Granja, M.; Albrecht, C.H.; Pires de Lima, B.S.L.; Jacob, B.P. *Incorporating Engineering Criteria to the Synthesis and Optimization of Submarine Pipeline Routes: On-Bottom Stability, Viv-Induced Fatigue and Multiphase Flow*; American Society of Mechanical Engineers Digital Collection: Lawrence, KS, USA, 2014.
25. de Lucena, R.R.; Baioco, J.S.; Pires de Lima, B.S.L.; Albrecht, C.H.; Jacob, B.P. Optimal Design of Submarine Pipeline Routes by Genetic Algorithm with Different Constraint Handling Techniques. *Adv. Eng. Softw.* **2014**, *76*, 110–124. [CrossRef]
26. Baioco, J.S.; Lima, M.; Albrecht, C.; Lima, B.; Jacob, B.; Rocha, D. Optimal Design of Submarine Pipelines by a Genetic Algorithm with Embedded On-bottom Stability Criteria. *Math. Probl. Eng.* **2018**, *2018*, 1781758. [CrossRef]
27. Kim, J.; Kwon, O.S.; Hai, N.L.D.; Ko, J.H. Study on the Design of an Underwater Chain Trencher via a Genetic Algorithm. *J. Mar. Sci. Eng.* **2019**, *7*, 429. [CrossRef]
28. Liu, D.-P.; Lin, T.-Y.; Huang, H.-H. Improving the Computational Efficiency for Optimization of Offshore Wind Turbine Jacket Substructure by Hybrid Algorithms. *J. Mar. Sci. Eng.* **2020**, *8*, 548. [CrossRef]
29. Ghigo, A.; Cottura, L.; Caradonna, R.; Bracco, G.; Mattiazzo, G. Platform Optimization and Cost Analysis in a Floating Offshore Wind Farm. *J. Mar. Sci. Eng.* **2020**, *8*, 835. [CrossRef]
30. Yin, D.; Niu, Y.; Yang, J.; Yu, S. Static and Discrete Berth Allocation for Large-Scale Marine-Loading Problem by Using Iterative Variable Grouping Genetic Algorithm. *J. Mar. Sci. Eng.* **2022**, *10*, 1294. [CrossRef]
31. Zhang, Y.; Diao, L.; Xu, C.; Zhang, J.; Wu, Q.; Pei, H.; Huang, L.; Li, X.; Qi, Y. An Optimization of New Energy Hybrid Configuration Parameters Based on GA Method. *J. Mar. Sci. Eng.* **2022**, *10*, 1747. [CrossRef]
32. Sun, Q.; Li, W.; Li, R.; Peng, D.; Guo, Q.; Zhao, Y.; Yue, Q.; Zhong, W. Anchor Chain Optimization Design of a Catenary Anchor Leg Mooring System Based on Adaptive Sampling. *J. Mar. Sci. Eng.* **2022**, *10*, 1739. [CrossRef]
33. Sun, H.; Yang, H.; Tao, S. Optimization of the Number, Hub Height and Layout of Offshore Wind Turbines. *J. Mar. Sci. Eng.* **2023**, *11*, 1566. [CrossRef]
34. Wilhoit, J.C.; Merwin, J.E. Pipe stresses induced in laying offshore pipeline. *J. Eng. Ind.* **1967**, *89*, 37–43. [CrossRef]
35. Dixon, D.A.; Rutledge, D.R. Stiffened catenary calculations in pipeline laying problem. *J. Eng. Ind.* **1968**, *90*, 153–160. [CrossRef]

36. Powers, J.T.; Finn, L.D. Stress analysis of offshore pipelines during installation. In Proceedings of the Offshore Technology Conference, Houston, TX, USA, 19–21 May 1969.
37. Wilkins, J.R. Offshore Pipeline Stress Analysis. In Proceedings of the Offshore Technology Conference (OTC 1227), Houston, TX, USA, 21–23 April 1970.
38. Palmer, A.C.; Hutchinson, G.; Ells, J.W. Configuration of submarine pipelines during laying operations, Transactions of ASME. *J. Eng. Ind.* **1974**, *96*, 1112–1118. [CrossRef]
39. Larsen, C.M.; Kavlie, D. Nonlinear analysis of oil pipelines by potential minimization. *Comput. Struct.* **1977**, *8*, 733–743. [CrossRef]
40. Malahy, R., Jr. Nonlinear Finite Element Method for the Analysis of the Offshore Pipe Laying Problem. Ph.D. Thesis, Rice University, Houston, TX, USA, 1985.
41. Yan, J.; Pedersen, P.T. 3-D Static Analysis of Pipelines during Laying. In Proceedings of the Offshore Technology Conference (OTC 5297), Houston, TX, USA, 5–8 May 1986.
42. Rienstra, S.W. Analytical approximations for offshore pipelaying problems. In Proceedings of the ICIAM, Paris, France, 6–9 July 1987.
43. Bernitsas, M.M.; Vlahopoulos, N. Three-dimensional nonlinear statics of pipelaying using condensation in an incremental finite element algorithm. *Comput. Struct.* **1990**, *35*, 195–214. [CrossRef]
44. Clauss, G.; Weede, H.; Saroukh, A. Nonlinear static and dynamic analysis of marine pipelines during laying. *Ship Technol. Res.* **1991**, *38*, 76–107.
45. Shin, H.; Kim, J.B.; Hara, S.; Yamakawa, K. Study of the Offshore Pipeline Installation Based on the Pipeline Experiment, Proceedings of the Sixth (1996). In Proceedings of the International Offshore and Polar Engineering Conference, Los Angeles, CA, USA, 26–31 May 1996.
46. Datta, T.K.; Basu, A.K. Stress analysis of submarine pipelines. *Proc. Inst. Civ. Engrs. Part 2* **1997**, *63*, 833–841. [CrossRef]
47. Guarracino, F.; Mallardo, V. A refined analytical analysis of submerged pipelines in seabed laying. *Appl. Ocean Res.* **1999**, *21*, 281–293. [CrossRef]
48. Lawinscky da Silva, D.M.; de Lima, M.H.A.; Jacob, B.P. Numerical model for the simulation of the pipeline-Laybarge interaction in pipelaying procedures. *Int. J. Model. Simul. Pet. Ind.* **2009**, *3*.
49. Li, Z.; Chen, Y.; Gong, S.; Jin, W. Configuration of Submarine Pipeline for Deepwater S-lay Technique. In Proceedings of the twentieth (2010) International Offshore and Polar Engineering Conference, Beijing, China, 20–25 June 2010.
50. Xu, P.; Du, Z.; Huang, F.; Javanmardi, A. Numerical Simulation of Deepwater S-lay and J-lay Pipeline Using Vector Form Intrinsic Finite Element Method. *Ocean Eng.* **2021**, *234*, 109039. [CrossRef]
51. Xu, P.; Ouyang, Z.H.; Du, Z.J.; Zhang, T.; Chen, B. Vector Form Intrinsic Finite Element Analysis of Deepwater J-laying Pipelines on Sloping Seabed. *Ocean Eng.* **2022**, *247*, 110709. [CrossRef]
52. Frisch-Fay, R. *Flexible Bars*; Butterworth: London, UK, 1962.
53. Mousselli, A.H. *Offshore Pipeline, Design, Analysis and Methods*; PenWell Publishing Company: Tulsa, OK, USA, 1981.
54. Bai, Y.; Bai, Q. *Subsea Pipeline Design, Analysis, and Installation 2014*; Elsevier: Amsterdam, The Netherlands, 2014.
55. Guo, B.; Song, S.; Chacko, J.; Ghalambor, A. *Offshore Pipelines*, 2nd ed.; Gulf Professional Publishing: Houston, TX, USA; Elsevier: Oxford, UK, 2014.
56. Jensen, G.A. Offshore Pipelaying Dynamics. PhD Thesis, NTNU, Trondheim, Norway, 2010.
57. Ivić, S. Sensitivity analysis of S-lay pipe-laying configuration. *Int. J. Appl. Eng. Res.* **2015**, *10*, 43250–43255.
58. Malahy, R., Jr. OFFPIPE User's Guide, Version 2.05, Houston. 1996. Available online: https://www.offpipe.com/download/manual.exe (accessed on 6 December 2023).
59. Orcina Ltd. Orcaflex. Available online: https://www.orcina.com/orcaflex/ (accessed on 6 December 2023).
60. John Wood Group Flexcom. Available online: https://www.woodplc.com/solutions/expertise/a-z-list-of-our-expertise/software-and-products/flexcom (accessed on 6 December 2023).
61. Dassault Systèmes SIMULIA Abaqus. Available online: https://www.3ds.com/products-services/simulia/products/abaqus/ (accessed on 6 December 2023).
62. Ansys Inc. Ansys Mechanical. Available online: https://www.ansys.com/products/structures/ansys-mechanical (accessed on 6 December 2023).
63. Autodesk Inventor Nastran. Available online: https://www.autodesk.com/products/inventor-nastran/overview (accessed on 6 December 2023).
64. Ivić, S.; Čanađija, M.; Družeta, S. Static Structural Analysis of S-lay Pipe Laying with a Tensioner Model Based on the Frictional Contact. *Eng. Rev.* **2014**, *34*, 223–234.
65. *DNV Standard DNV-ST-F101*; Submarine Pipeline Systems, Edition August 2021. Amended December 2021. DNV: Høvik, Norway, 2021.
66. RAO, S.S. *Engineering Optimization*; Wiley & Sons: New York, NY, USA, 1996.
67. Goldberg, D.E. *Genetic Algorithms in Search, Optimisation and Machine Learning*; Addison-Wesley Inc.: Boston, MA, USA, 1989.
68. Gen, M.; Cheng, R. *Genetic Algorithms and Engineering Design*; Wiley & Sons: New York, NY, USA, 1997.
69. Gen, M.; Cheng, R. *Genetic Algorithms and Engineering Optimization*; Wiley & Sons: New York, NY, USA, 2000.
70. Sivanandam, S.N.; Deepa, S.N. *Introduction to Genetic Algorithms*; Springer: Berlin/Heidelberg, Germany, 2008.
71. Haupt, R.L.; Haups, S.E. *Practical Genetic Algorithms*; John Wiley & Sons: Hoboken, NJ, USA, 2004.

72. Michalewicz, Z.; Schoenauer, M. Evolutionary Algorithms for Constrained Parameter Optimization Problems. *Evol. Comput.* **1996**, *4*, 1–32. [CrossRef]
73. Yeniay, Ö. Penalty Function Methods for Constrained Optimization with Genetic Algorithms. *Math. Comput. Appl.* **2005**, *10*, 45–56. [CrossRef]

Disclaimer/Publisher's Note: The statements, opinions and data contained in all publications are solely those of the individual author(s) and contributor(s) and not of MDPI and/or the editor(s). MDPI and/or the editor(s) disclaim responsibility for any injury to people or property resulting from any ideas, methods, instructions or products referred to in the content.